

DEVELOPMENT OF QUANTUM DOT-BASED LIVE-CELL PHARMACOLOGICAL  
ASSAYS AIMED AT MEMBRANE TRANSPORTERS AND RECEPTORS

By

Emily Jones Ross

Thesis

Submitted to the Faculty of the  
Graduate School of Vanderbilt University  
in partial fulfillment of the requirements

for the degree of

MASTER OF SCIENCE

in

Chemistry

May, 2013

Nashville, Tennessee

Approved:

Professor Sandra J. Rosenthal

Professor Eva M. Harth

## ACKNOWLEDGEMENTS

I appreciate the help of my advisor, Dr. Sandy Rosenthal, and all of the wonderful people in the Chemistry Department that contributed to my graduate career. During my time in the Rosenthal lab, my colleagues ensured I was constantly engaged and entertained along the way. Specifically, I would like to thank Dr. Jerry “Super Student” Chang and Oleg “Mr. Pibb” Kovtun for their advice on these projects and their assistance in teaching me the foundations of research and critical thinking. I am very proud and honored to be included into the beloved sub-group called, “the bio-side”. I would also like to thank Dr. James “Historian” McBride, Dr. Melissa Harrison, Dr. Rebecca Sandlin, Holly Carrell, and Chris Gulka for their helpful discussions and guidance in areas where I was not as knowledgeable. In particular, I cannot be thankful enough for exceptional friendships I have experienced in graduate school. The musical concerts, Mellow Mushroom happy hours, TA “therapy” sessions, breakfast/lunch/dinner/coffee breaks, and the encouraging words with smiles have made graduate school bearable. Also, a special thanks to those who helped me with data acquisition and advice, specifically Kasia Derewacz and Dr. M. Wade Calcutt with their help with the somatostatin project.

Outside of the lab, plenty of people kept me sane and happy. My best friend and husband, Craig, has been supportive, patient, and loving through this crazy graduate school experience. I love him dearly! My loving family has been consistent rock of support; they always make sure I feel their confidence and encouragement from afar. Mama, one thesis down, one more to go! From my lap or closely watching from the sofa, Bailey, Zoey, and Bob closely supervised the writing of many paragraphs of this thesis (thanks for the needed interruptions, animal babies). A big thank you goes out to all of my Huntsville friends near and far. Most importantly, I could have not have completed any of this work without the help of my Lord and Savior. He is the reason I survived and made it through to the other side (Philippians 4:13).

This work would not have been financially possible without the support of Vanderbilt University, National Institutes of Health GM72048-02, and the Vanderbilt Institute of Chemical Biology.

## TABLE OF CONTENTS

	Page
ACKNOWLEDGEMENTS .....	ii
LIST OF FIGURES .....	v
LIST OF TABLES .....	viii
LIST OF EQUATIONS .....	ix
Chapter	
I. QUANTUM DOT FLOW CYTOMETRY IN STRUCTURE-ACTIVITY RELATIONSHIP STUDY OF OPTIMIZED HUMAN SEROTONIN TRANSPORTER LIGANDS.....	1
INTRODUCTION .....	1
EXPERIMENTAL.....	4
RESULTS AND DISCUSSION.....	14
CONCLUSION AND FUTURE DIRECTIONS.....	19
II. QUANTUM DOT FLUORESCENCE-BASED DRUG DISCOVERY	
Human Serotonin Transporter Displacement Assay .....	20
INTRODUCTION .....	20
EXPERIMENTAL.....	24
RESULTS AND DISCUSSION.....	27
CONCLUSION AND FUTURE DIRECTIONS.....	31
Human Dopamine Transporter Medium-Throughput Flow Cytometry Screening Method	
INTRODUCTION .....	32
EXPERIMENTAL.....	35

RESULTS AND DISCUSSION .....	39
CONCLUSION AND FUTURE DIRECTIONS .....	44
III. DEVELOPMENT OF A QUANTUM DOT-BASED FLUORESCENT SOMATOSTATIN RECEPTOR PROBE .....	45
INTRODUCTION .....	45
EXPERIMENTAL .....	47
RESULTS AND DISCUSSION .....	50
CONCLUSION AND FUTURE DIRECTIONS .....	57
Appendix	
A. LIGAND IDT567, IDT571, AND IDT576 SCREENING PROCESS .....	59
B. IDT318 SYNTHESIZED JULY 22, 2011 AND SCREENED SEPT.-OCT., 2011 .....	67
C. PRELIMINARY PERKIN ELIMER OPERA IMAGING .....	74
REFERENCES .....	77

## LIST OF FIGURES

	Page
1. Structures of the 3-(1,2,3,6-tetrahydropyridin-4-yl)-1H-indole ligands and its cyano derivative, 3-(1,2,3,6-tetrahydropyridin-4-yl)-1H-indole-5-carbonitrile ligands .....	4
2. Demonstrative modeling data of IDT318 parent drug .....	5
3. Images of hSERT-HEK293T or HEK293T cells exposed to fluorescent compound, IDT307 .....	7
4. Representative images of hSERT-HEK293T or HEK293T cells exposed to two-step QD labeling protocol .....	9
5. Schematic of a QD-based assay .....	11
6. The heat map and representative histogram plots of the effects of increasing the alkyl spacer length .....	13
7. The table details all of the average percent fluorescent intensity values of each of the ligands screened .....	16
8. Visualization of the trend of average percent fluorescent intensity values of each of the ligands screened compared to alkyl spacer length.....	17
9. RosettaScore Modeling data compared to the alkyl spacer length .....	18
10. Diagram of QD Based SERT displacement assay .....	23
11. Schematic of Qdot nanoconjugates for SERT labeling .....	24
12. The absorption and fluorescence emission spectra of Qdot® streptavidin conjugate is diagrammed .....	26
13. Stably transfected hSERT HEK-293T cells treated with 0.5 $\mu$ M of IDT318 ligand.....	28
14. Diagrams of drug analogues of ligands IDT361 and IDT318 .....	28
15. Stably transfected hSERT HEK-293T cells treated with 0.5 $\mu$ M IDT361 .....	29
16. Time-dependent fluorescent intensity plot.....	30

17.	Schematic of Qdot nanoconjugates for DAT labeling .....	35
18.	Labeling method of Qdot nanoconjugates for DAT proteins .....	38
19.	Images of Flip In hDAT HEK293 cells exposed to two-step SavQD655 labeling.....	40
20.	Statistical evaluation, or Z' factor, of QD-DAT assay .....	41
21.	Dose-response screening of GBR12909 .....	43
22.	Solid Phase Peptide Synthesis diagram .....	48
23.	Schematic of Qdot nanoconjugates for Somatostatin receptor (SSTR) labeling.....	50
24.	Biotinylated end of the Ala serves as the binding site for the Streptavidin-Quantum Dots.....	51
25.	Optical ultraviolet (UV) absorbance of peptides and peptide probes .....	53
26.	Liquid Chromatography-Electrospray Ionization-Mass Spectrometry (LC-ESI MS) predicted molecular weights for the Somatostatin-14 control .....	54
27.	Liquid Chromatography-Electrospray Ionization-Mass Spectrometry (LC-ESI MS) predicted molecular weights for SST-14 peptide and Somatostatin-14-Lys(Biotin) probe.....	55
28.	Diagram of Ellman's assay .....	56
29.	Graph of cysteine standard curve used for the Ellman's assay.....	56
A-1.	Ligands IDT567, IDT571, and IDT576 .....	60
A-2.	Experimental sample 24-well plate.....	61
A-3.	IDT307 fluorescence assay .....	64
A-4.	Ligands IDT567, IDT571, and IDT576 flow cytometry and microscopy images .....	66
B-1.	Experimental sample 24-well plate.....	68
B-2.	IDT307 fluorescence assay .....	70
B-3.	IDT318 flow cytometry and microscopy images at 20x.....	71

B-4.	IDT318 microscopy images at 100x .....	72
C-1.	Perkin Elmer Opera Image.....	76

## LIST OF TABLES

	Page
1. Results from the Ellman's assay .....	57



## LIST OF EQUATIONS

	Page
1. $Z'$ statistical factor .....	39
2. Percent Inhibition (PI).....	42

## Chapter I

### Quantum Dot Flow Cytometry in Structure-Activity Relationship Study of Optimized Human Serotonin Transporter Ligands

#### INTRODUCTION

Major depression is a debilitating and recurrent disorder with a substantial lifetime risk and a high social cost.<sup>1</sup> At any given time, depression has been shown to affect nearly 18 million people in the United States alone.<sup>2</sup> Over the past 30 years, numerous studies of the serotonin (5-Hydroxytryptophan, 5-HT) system and one of its principal components, serotonin transporter (SERT) protein, have reinforced the significant role of the serotonergic pathway in pathophysiology of major depression.<sup>3</sup> In particular, disrupted SERT cellular localization and regulation have been implicated in multiple neuropsychiatric disorders, including anxiety, depression and autism.<sup>1,3</sup> The presynaptic serotonin transporter regulates synaptic levels of 5-HT by recycling it into the presynaptic terminals in the brain.<sup>4</sup> Low synaptic 5-HT levels have been shown to induce depressive symptoms, such as mood swings, fatigue, anxiety, and suicidal tendencies. To treat these symptoms, selective serotonin reuptake inhibitors (SSRIs) are widely used as clinical antidepressants. One of the major challenges associated with the discovery of new, more efficacious antidepressants is the lack of a resolved crystal structure of the serotonin transporter. At present, methods to investigate SERT activity include mainly conventional biochemical and radiolabeling approaches such as phosphorylation assays, electrophysiology, or radio-isotope substrate uptake assays.<sup>5</sup> The disadvantages of these

methods include time-consuming, labor-intensive experimental work, poor spatiotemporal resolution, and safety concerns associated with isotope handling.<sup>1</sup>

As an alternative, fluorescent probes can be used for target selective drug screening of membrane transporter proteins. The live-cell labeling, tracking and dynamic investigations of hSERT, and other membrane proteins, pose complications when studied due to important challenges. Typically, antibody-based labeling approach is utilized to detect single membrane proteins;<sup>6-7</sup> however, many proteins lack suitable extracellular domains that can be targeted by antibodies without functional disruption. Furthermore, the use of popular fusion tags to label membrane proteins, usually consisting of a short peptide sequence with a recognition epitope for a complementary binding partner, such as hemagglutinin (HA), requires genetic perturbation of the protein target<sup>8</sup> and thus does not allow direct visualization of endogenous protein of interest.

The Rosenthal group has pioneered the use of organic ligands conjugated to quantum dots to target cell surface membrane proteins.<sup>9,10</sup> Organic ligands can achieve specific targeting of transporter proteins, which allows visualization of endogenous protein without the functional disruption of the protein of interest. Quantum dots (QDs), nanometer-sized semiconductor nanocrystals, exhibit excellent photostability and brightness, which allow for long-term imaging of biological systems.<sup>9,10</sup> Also, their broad absorption spectra and size-dependent, narrow, symmetric emission spectra of QDs considerably simplify multiplexed, molecular imaging experiments. Based on the structure of the cell surface protein, the organic ligand can be tailored with a linker arm to optimize QD conjugate binding to the target protein.<sup>8,10</sup> The ability to find the structural requirements for optimal binding activity can be achieved by molecular modeling. The

molecular modeling of an organic ligand saves time by eliminating unnecessary organic chemistry synthesis and reveals an optimized ligand design for the protein of interest.

Even though, the serotonin transporter crystal structure has not been determined, a homology model has been created based upon the crystal structure of LeuTaq as a template.<sup>11-13</sup> The homology model of hSERT provides a structure to computationally dock ligands with RosettaLigand.<sup>11-13</sup> In the following structure-activity relationship study, we have investigated how subtle modifications of the selected SERT ligands can lead to dramatic changes in binding affinity and selectivity towards the SERT protein. Recently, we reported the synthesis of probes of the human serotonin transporter where an alkyl spacer was attached to high affinity SERT antagonist, followed by the subsequent conjugation of a biotinylated, polyethylene glycol chain.<sup>14</sup> These synthesized SERT ligands are amenable to conjugation to streptavidin coated QDs via the biotin-streptavidin binding interaction. The affinities of these SERT ligands were measured by their ability to produce SERT-dependent currents in *Xenopus laevis* oocytes. Even though these SERT ligands were found to bind to the SERT protein of interest, no insight into the ideal alkyl space in linker arm needed for the SERT membrane protein binding has been provided.

Here, RosettaLigand computer modeling software provides insight into the structural-activity relationship of SERT protein and would allow for faster optimized ligand design of an ideal alkyl space in linker arm. RosettaLigand is a premiere algorithm that has proven successful docking of ligands into crystal structures. The RosettaLigand program rapidly docks multiple conformations of ligands into crystal structures. This process can be used in conjunction with the homology hSERT model to

dock known substrates and inhibitors. In this study, 3-(1,2,3,6-tetrahydropyridin-4-yl)-1H-indole and its cyano derivative, 3-(1,2,3,6-tetrahydropyridin-4-yl)-1H-indole-5-carbonitrile, have been docked into the homologous model of hSERT using RosettaLigand. Using docking studies of the SERT model, we investigated the length of alkyl spacer in the linker arm of the organic ligands, using 2, 6, 7, 8, or 11 alkyl spacer lengths, and the effect of binding in both ligand models (Figure 1).

To validate the modeling, QD flow cytometry-based assay measuring

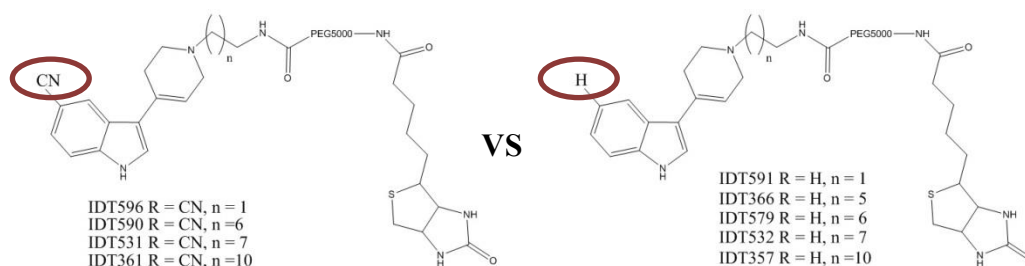


Figure 1. Structures of the 3-(1,2,3,6-tetrahydropyridin-4-yl)-1H-indole ligands and its cyano derivative, 3-(1,2,3,6-tetrahydropyridin-4-yl)-1H-indole-5-carbonitrile ligands.

fluorescence of ligand binding was done to demonstrate and confirm that structural modeling can optimize length of the organic ligand linker arm design and synthesis.

## EXPERIMENTAL

### RosettaLigand Computer Modeling

Parent drugs were designed using the Molecular Environment (MOE) 2009 application. Ten conformations were generated for each drug with an RMSD  $\geq 0.5\text{\AA}$ . The parent drug was then placed in the binding pocket of hSERT overlapping the known binding site of 5-HT. The ligand was then docked using RosettaLigand confined to 5\text{\AA} movement from its initial location, generating 5000 output complexes. The top ten

scoring complexes, based on the overall RosettaLigand score, were used for further evaluation.

An alkyl spacer was built one carbon at a time, spanning from one to eleven carbons, by sequentially adding one methyl group to the N-terminus of the ligand. Ten conformations were generated for each ligand by holding the previously docked complex in place (only the newly added methyl group was allowed to move freely for conformation generation). The compounds were then docked using RosettaLigand confined to 1.5Å of their original location in the binding pocket, generating 5000 output complexes per ligand. The top five scoring complexes were then evaluated and used in sequential alkyl spacer addition.

In order to determine whether or not the alkyl spacer of the ligand accurately spans the hydrophobic region of hSERT, a heatmap of the protein was generated. This heat map scores each residue of the protein and, among other things, predicts which region of the protein (hydrophobic, transition or hydrophilic) the residue is most likely to

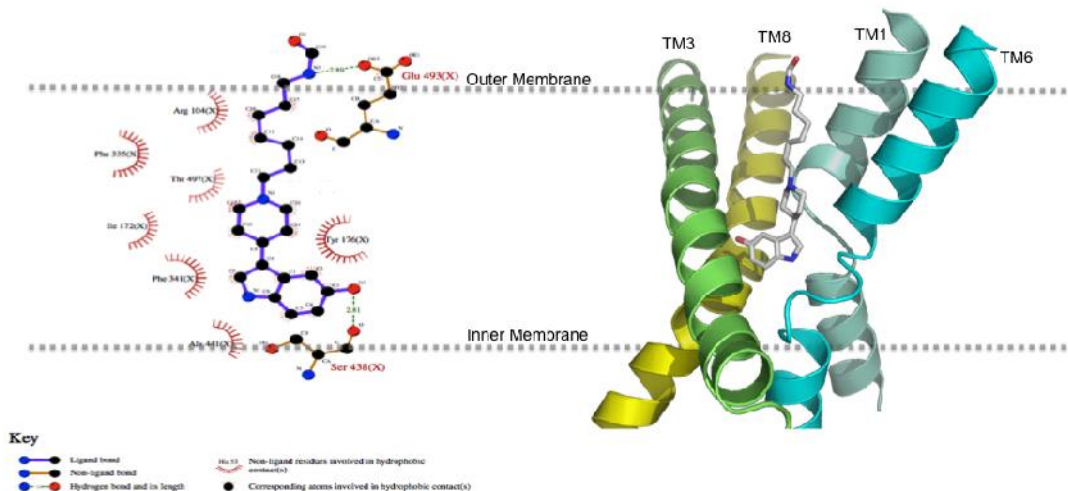


Figure 2. Demonstrative modeling data of IDT318 parent drug attached to a seven-carbon alkyl spacer reaches residues 103, 104, and 179, suggesting it accurately spans the hydrophobic region.

reside in. Residues predicted to be in the transition region of the protein were used to generate a plane which served as the protein's transition region. The residues chosen were Arg104, Ile179, and Tyr495 (Figure 2).

### **Cell Line Maintenance and hSERT Activity Assay**

The hSERT stably transfected HEK293T host cell line was provided by Dr. Randy Blakely's lab (Vanderbilt University) and was grown in complete DMEM, supplemented with 10% dialyzed FBS and incubated in humidified atmosphere with 5% CO<sub>2</sub> at 37°C. The SERT-expressing HEK293T cells were selected in the presence of 400 µg/mL G418.

The SERT protein activity in living HEK293T cells was examined before each experiment by using IDT307, a fluorescent neurotransmitter substrate.<sup>15</sup> IDT307 compound is nonfluorescent in solution but fluoresces as the substrate is accumulated into the nucleus membrane, affording real-time evaluation of SERT uptake activity.<sup>15</sup> The assay to verify successful SERT expression in HEK293T cells involves the addition of IDT307 directly to the culture media at a final concentration of 5 µM and incubating at 37°C for 10 minutes. Fluorescent images were then acquired immediately after IDT307 addition, and successful transporter expression was evident by an observable increase in intracellular fluorescence (see Figure 3).

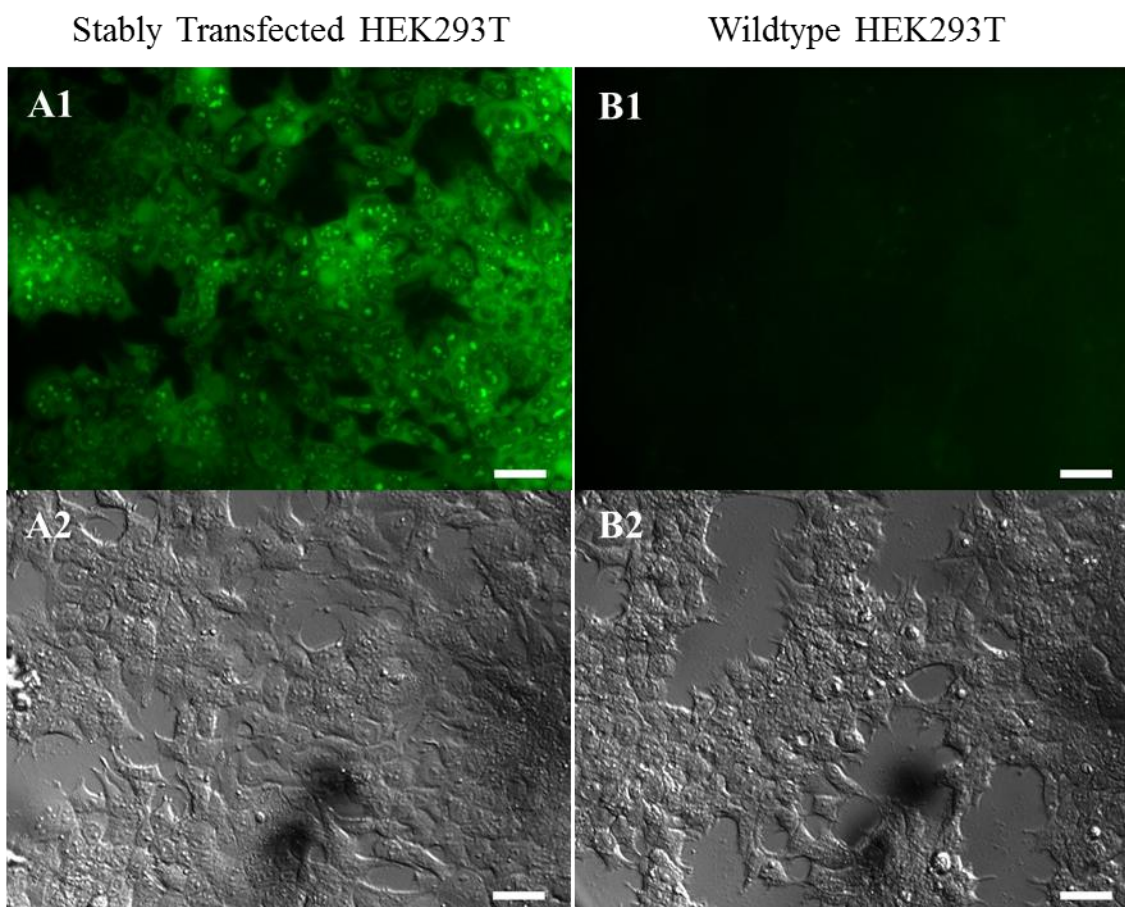


Figure 3. Images of hSERT-HEK293T or HEK293T cells exposed to fluorescent compound, IDT307. Representative images are shown for the stably transfected hSERT-HEK293T cells (A1, A2) and HEK293T (Wildtype) cells (B1, B2). All samples were treated with 5  $\mu$ M IDT307, a fluorescent neurotransmitter substrate, and incubated at 37°C for 10 minutes. Fluorescent (top) and DIC (bottom) images are shown. Calibration Bar = 40 $\mu$ m

### **Labeling HEK293T Cells with Ligand-Conjugated Quantum Dots for Fluorescent Microscopy**

The stably transfected hSERT-expressing HEK293T cells were treated using a two-step quantum dot, Qdot® 655 streptavidin conjugate (Invitrogen™), labeling protocol. Previously before flow cytometry experiments, SERT-expressing HEK293T cells were seeded MatTek (MetTek Corporation) polylysine-coated plates and were allowed to grow for approximately 48hours at 37°C and 5%CO<sub>2</sub>.



Adherent SERT-expressing (1) competition control cells were pre-blocked by exposure to 10  $\mu$ M of Paroxetine and incubated for 10 minutes at 5% CO<sub>2</sub> / 37°C, (2) competition control, wild type, and positive cells were incubated with 0.5 $\mu$ M SERT ligands with inhibitor mixture for 10 min for all sample types, (3) washed several times with DMEM free media and incubated with 1 nM SavQD655/1% BSA (bovine serum albumin) mixture, (4) After the SavQD655 labeling step, HEK cells were washed with DMEM free media to remove any unbound SavQD655 and cells images were acquired on the Zeiss Laser Scanning Microscope 510 inverted confocal microscope. Representative images of hSERT-HEK293T or HEK293T cells exposed to two-step QD labeling protocol using the ligand, IDT357 can be seen in Figure 4.

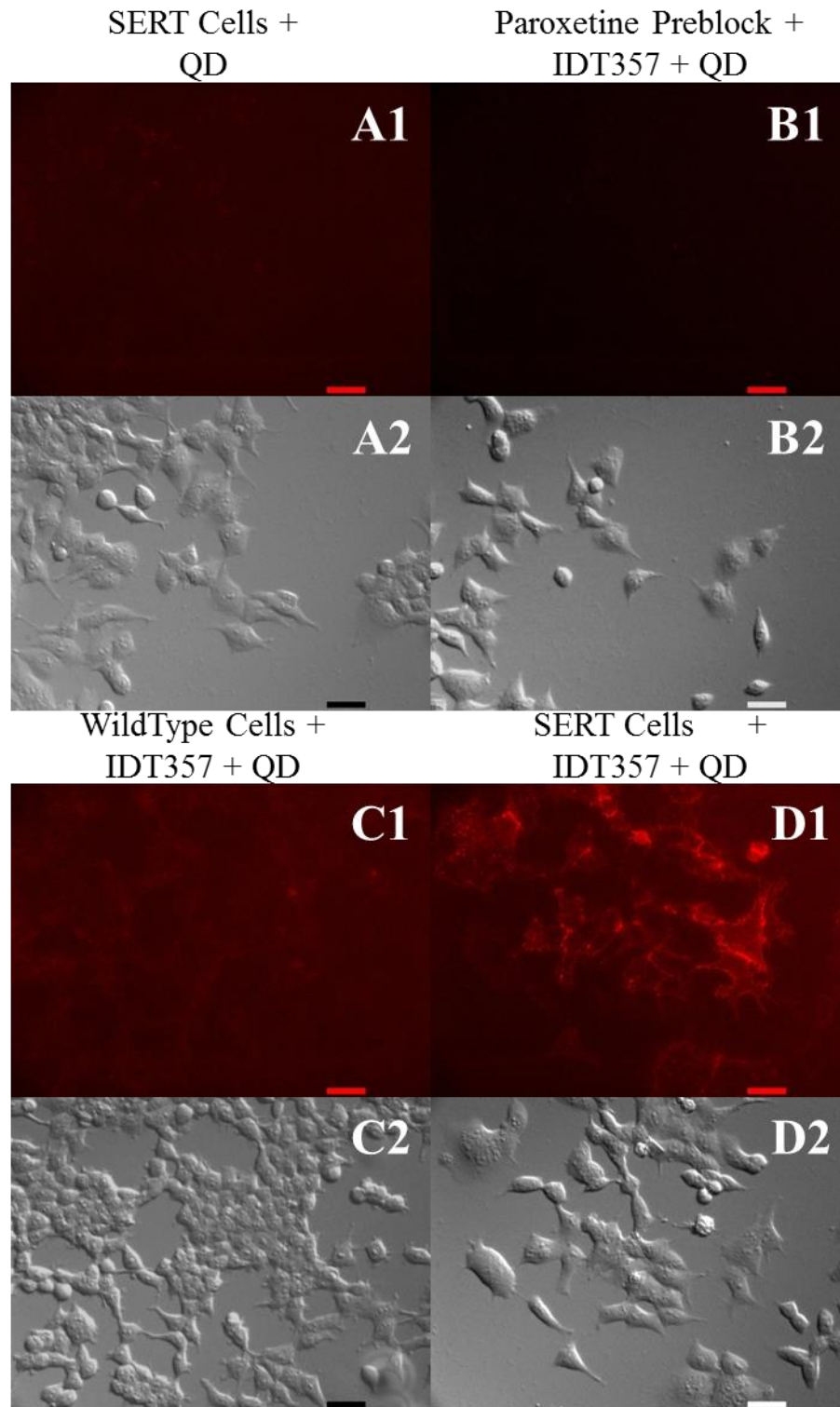


Figure 4. Representative images of hSERT-HEK293T or HEK293T cells exposed to two-step QD labeling protocol using the ligand, IDT357. SavQD655 labeling of hSERT stably expressed in HEK293T cells (A1 – D2) and HEK293T (Wildtype) cells (C1, C2). Compared to QD only control (A1, A2), Paroxetine pre-block competition (B1, B2), and Wild Type cells (C1, C2), the fluorescent intensity increased with hSERT-HEK293T IDT357 positively labeled cells. Fluorescent (top) and DIC (bottom) images are shown. Calibration Bar = 40um

## **Labeling HEK293T Cells with Ligand-Conjugated Quantum Dots for Flow Cytometry**

The stably transfected hSERT-expressing HEK293T cells were treated using a two-step quantum dot, Qdot® 655 streptavidin conjugate (Invitrogen™), labeling protocol. Previously before flow cytometry experiments, SERT-expressing HEK293T cells were seeded in 24-well polylysine-coated plates (BD Bioscience®) and were allowed to grow for approximately 48hours at 5% CO<sub>2</sub> / 37°C.

Next, a flow cytometry-based probe screening protocol was established that would allow multi-well plate screening of both adherent and suspension cell cultures using our ligand-conjugated SavQDs. The screening platform is depicted in Figure 5. Adherent SERT-expressing (1) competition control cells were pre-blocked by exposure to 10 µM of Paroxetine, a potent and selective serotonin reuptake inhibitor (SSRI), and incubated for 10 minutes at 5% CO<sub>2</sub> / 37°C, (2) competition control, wildtype, and positive cells were incubated with 0.5µM SERT ligands with inhibitor mixture for 10 min for all sample types, (3) washed several times with DMEM free media and incubated with 1 nM SavQD655/1% BSA (bovine serum albumin) mixture, (4) nonenzymatically dissociated (Cellstripper™), and (5) assayed by flow cytometry. Before each fluorescence measurement are obtained, the voltage of the 5-laser BD LSRII cytometer are adjusted by using Attune™ Performance tracking or calibration beads (Applied Biosystems®).

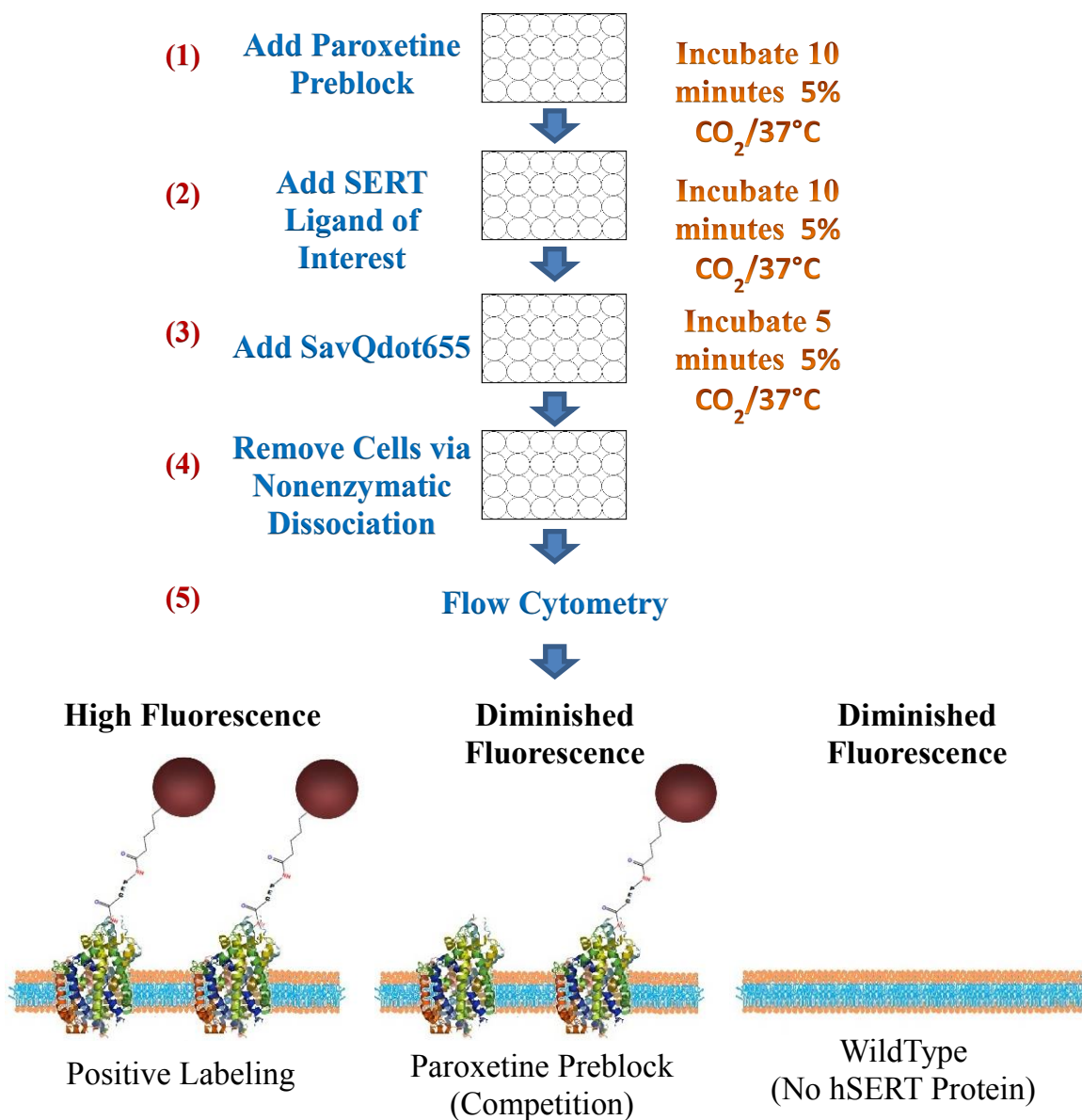
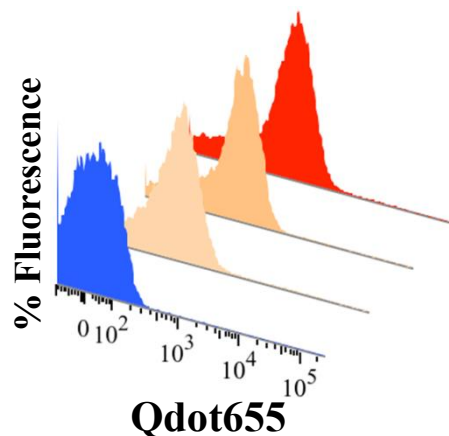


Figure 5. Schematic of a QD-based assay that investigates the length of alkyl spacer in the linker arm of the organic ligands, using 2, 6, 7, 8, or 11 alkyl spacer lengths, and the effect of binding in ligand models. Adherent SERT-expressing (1) competition control cells were exposed to 10  $\mu\text{M}$  of Paroxetine, a potent and selective serotonin reuptake inhibitor (SSRI), and incubated for 10 minutes at 5% CO<sub>2</sub> / 37°C, (2) competition control, wildtype, and positive cells were incubated with 0.5  $\mu\text{M}$  SERT probes with inhibitor mixture for 10 min for all sample types, (3) washed several times with DMEM free media and incubated with 1 nM SavQD655/1% BSA (bovine serum albumin) mixture, (4) nonenzymatically dissociated (Cellstripper™), and (5) assayed by flow cytometry.

Obtained fluorescence percent data were pooled from five independent experiments with triplicate samples to generate average percent fluorescent intensities of each of the cyano group ligands or indole (hydrogen) ligands (Figure 1). The heat map, representative histogram plots, and data tables were generated using average percent fluorescent intensity values pooled from five independent experiments with triplicate samples of each ligand subtype (Figure 6).

### 3-(1,2,3,6-tetrahydropyridin-4-yl)-1H-indole-5-carbonitrile Ligands

Alkyl Spacer Length	2	7	8	11
Positive Samples	Blue	Orange	Orange	Red
Paroxetine Preblock	Blue	Yellow	Yellow	Yellow
Wild Type	Grey	Orange	Orange	Orange



### 3-(1,2,3,6-tetrahydropyridin-4-yl)-1H-indole Ligands

Alkyl Spacer Length	2	6	7	8	11
Positive Samples	Blue	Orange	Yellow-Orange	Orange	Red
Paroxetine Preblock	Blue	Blue	Blue	Grey	Grey
Wild Type	Yellow	Yellow	Orange	Orange	Orange

	SERT Cells	SERT Cells + QDs	WildType Cells	WildType Cells + QDs
Control	Blue	Blue	Blue	Blue

#### Percent Fluorescence

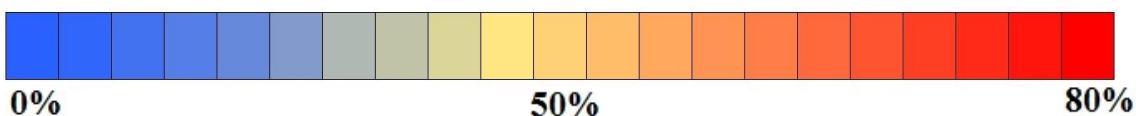


Figure 6. Screening of stably transfected hSERT-expressing HEK293T cell line to investigate the effect of length of alkyl spacer in the linker arm, using 2, 6, 7, 8, or 11 alkyl spacers. The heat map and representative histogram plots of the effects of increasing the alkyl spacer length on QD conjugate binding are shown. The heat map and representative histogram plots were generated using average percent fluorescent intensity values pooled from five independent experiments with triplicate samples of each ligand subtype.

## RESULTS AND DISCUSSION

The stably transfected hSERT-expressing HEK293T cell line was used as a model system to investigate the effect of the length of alkyl spacer in the linker arm on binding, using 2, 6, 7, 8, or 11 alkyl spacer lengths. The effect length of alkyl spacer in the linker arm on ligand binding were compared in both ligand models containing the 3-(1,2,3,6-tetrahydropyridin-4-yl)-1H-indole drug end and its cyano derivative ligand, 3-(1,2,3,6-tetrahydropyridin-4-yl)-1H-indole-5-carbonitrile.

The serotonin transporter expression level in living HEK293T cells was examined before each flow cytometry experiment by using IDT307, a fluorescent monoamine neurotransmitter transporter substrate. Representative images of hSERT-HEK293T or HEK293T cells after exposure to IDT307 are shown in Figure 3. Intracellular accumulation of IDT307 by functional membrane SERTs (Figure 3:A1, A2) resulted in a characteristic mitochondria- and nucleoli-associated fluorescence. In contrast, the HEK293T (Wildtype) cells (Figure 3:B1, B2) demonstrated no such fluorescence.

Both hSERT-expressing HEK293T and wildtype cells were subjected to a two-step QD labeling protocol and SERT QD labeling was demonstrated by techniques microscopy and flow cytometry. The representative histogram plots and heat map of the effects of increasing the alkyl spacer length on QD conjugate binding are shown in Figure 6. Comparison of control samples (QD only treated cells, Paroxetine pre-block and wildtype cells); the increase of average percent fluorescent intensity is closely correlated with the alkyl spacer length. This correlation can also be seen in the presence of membrane-associated QD fluorescent labeling on the acquired microscopy images (Figure 4). SavQD655 labeling of hSERT is demonstrated in stably expressing

HEK293T cells (Figure 4:A1 – D2) and HEK293T (Wildtype) cells (Figure :C1, C2). Compared to QD only control (Figure 4:A1, A2), Paroxetine pre-block competition (Figure 4:B1, B2), and Wild Type cells (Figure 4:C1, C2), the fluorescent intensity increased with hSERT-HEK293T IDT357 positively labeled cells. A detailed depiction of all of the average percent fluorescent intensity values can be seen in Table and in Figure 7. These data demonstrate that our QD-based approach can be used to investigate the length of alkyl spacer in the linker arm in a living cell assay.



### 3-(1,2,3,6-tetrahydropyridin-4-yl)-1H-indole-5-carbonitrile Ligands

	Average Standard Error of the Mean (SEM)
SERT Cells	0.147 ± 0.026
SERT Cells + QD	3.086 ± 0.657
WildType + Cells	0.165 ± 0.060
WildType + QD	1.096 ± 0.314

SERT Cells + IDT596	7.384 ± 2.207
Paroxetine Preblock + IDT596	3.060 ± 0.565
WildType + IDT596	12.061 ± 2.702

SERT Cells + IDT590	48.538 ± 8.610
Paroxetine Preblock + IDT590	22.557 ± 11.487
WildType + IDT590	32.887 ± 6.449

SERT Cells + IDT531	42.866 ± 8.487
Paroxetine Preblock + IDT531	22.386 ± 8.508
WildType + IDT531	37.810 ± 7.645

SERT Cells + IDT361	75.090 ± 3.783
Paroxetine Preblock + IDT361	26.035 ± 10.383
WildType + IDT361	40.731 ± 7.888

### 3-(1,2,3,6-tetrahydropyridin-4-yl)-1H-indole Ligands

	Average Standard Error of the Mean (SEM)
SERT Cells	0.147 ± 0.026
SERT Cells + QD	3.086 ± 0.657
WildType + Cells	0.165 ± 0.060
WildType + QD	1.096 ± 0.314

SERT Cells + IDT591	6.230 ± 0.790
Paroxetine Preblock + IDT591	4.295 ± 0.375
WildType + IDT591	20.750 ± 0.563

SERT Cells + IDT366	34.100 ± 5.000
Paroxetine Preblock + IDT366	5.015 ± 0.455
WildType + IDT366	21.825 ± 0.891

SERT Cells + IDT579	30.150 ± 4.050
Paroxetine Preblock + IDT579	6.960 ± 0.330
WildType + IDT579	29.100 ± 1.578

SERT Cells + IDT532	53.750 ± 4.846
Paroxetine Preblock + IDT532	11.555 ± 4.272
WildType + IDT532	32.671 ± 9.156

SERT Cells + IDT357	73.625 ± 5.951
Paroxetine Preblock + IDT357	10.898 ± 3.165
WildType + IDT357	37.936 ± 9.778

Figure 7. The table details all of the average percent fluorescent intensity values of each of the ligands screened. SavQD655 labeling of hSERT stably expressed in HEK293T cells and HEK293T (Wildtype) cells.

Visualization of the trend between the average percent fluorescent intensity values and the carbon alkyl spacer length can be seen in Figure 8. As the carbon alkyl spacer length increased in both ligand models containing the 3-(1,2,3,6-tetrahydropyridin-4-yl)-1H-indole drug end and its cyano derivative ligand, 3-(1,2,3,6-tetrahydropyridin-4-yl)-1H-indole-5-carbonitrile, the average percent fluorescent intensities increased (Figures 8: A, B). The ideal binding length from RosettaLigand modeling predicted that an alkyl spacer greater than six would provide sufficient labeling (Figure 9).

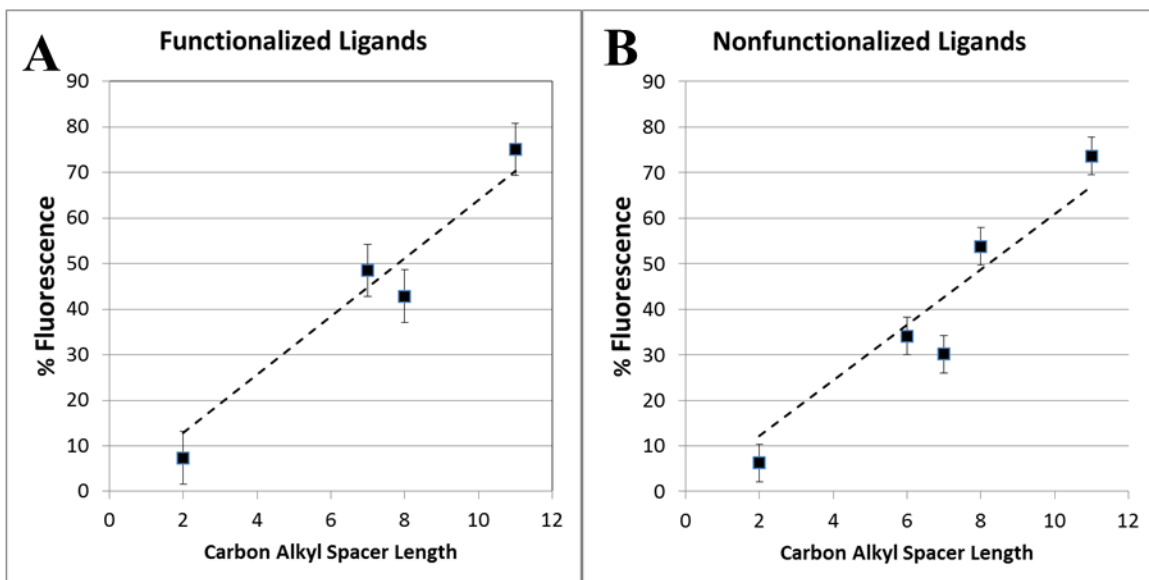


Figure 8. Visualization of the trend of average percent fluorescent intensity values of each of the ligands screened compared to alkyl spacer length

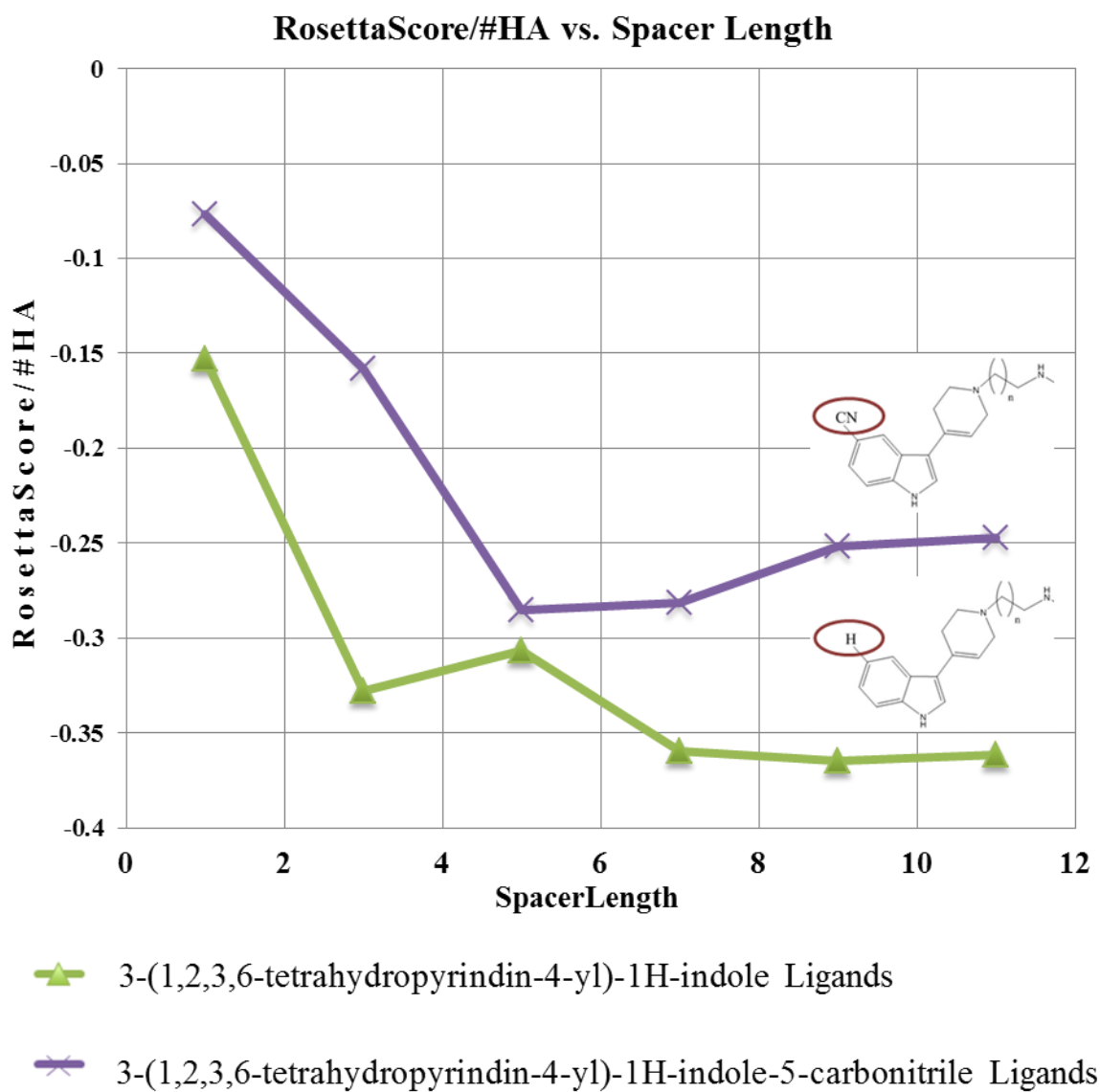


Figure 9. RosettaScore Modeling data compared to the alkyl spacer length

## **CONCLUSION AND FUTURE DIRECTIONS**

These flow cytometry fluorescent intensity results are in good agreement with the trend obtained by the predictions with RosettaLigand and the RosettaScore software. According to the RosettaLigand calculations, as the alkyl spacer length increased in both ligand models, the binding affinity for the SERT protein increased, with the 6-carbon alkyl spacer being the minimum length to maximize binding affinity of the SERT ligand. Based on these findings, one can combine molecular modeling and fluorescence-based assays to improve ligand design and development.

## **Chapter II**

### **Quantum Dot Fluorescence-Based Drug Discovery**

#### **A. Human Serotonin Transporter Displacement Assay**

##### **INTRODUCTION**

Major depression is a debilitating and recurrent disorder with a substantial lifetime risk and a high social cost.<sup>1</sup> At any given time, depression has been shown to affect nearly 18 million people in the United States alone.<sup>2</sup> Over the past 30 years, a variety of studies of the serotonin (5-Hydroxytryptophan, 5-HT) system and its principal component, serotonin transporter (5-HT, SERT), have reinforced its significant role in pathophysiology of major depression.<sup>3</sup> The presynaptic serotonin transporter regulates synaptic levels of 5-HT by recycling it into the presynaptic terminals in the brain.<sup>4</sup> Low synaptic 5-HT levels have been shown to induce depressive symptoms, such as mood swings, fatigue, anxiety, and suicidal tendencies.<sup>1</sup> To treat these symptoms, selective serotonin reuptake inhibitors (SSRIs) are widely used as clinical antidepressants. One of the major drawbacks of antidepressants is the delayed onset of clinical effect, which can take as long as 3-6 weeks.<sup>16</sup> Within the past decade, a number of new antidepressant agents have been developed that act on multiple targets, such as serotonin-norepinephrine reuptake inhibitors (SNRIs) and the serotonin-norepinephrine-dopamine reuptake

inhibitors (SNDRIs).<sup>2</sup> SNRIs and SNDRIs have been reported to possess a slightly greater efficacy and possibly a more rapid onset of action, than SSRIs.<sup>1</sup> Another emerging area in antidepressant drug discovery focuses on studying the primary binding pocket (orthosteric site) of SERT versus the secondary, allosteric binding site of the protein. Currently, no crystal structure of the serotonin transporter protein is available, which makes validating allosteric or orthosteric antagonism difficult.<sup>17,18</sup> A number of potent SSRIs have been proposed as allosteric modulators for SERT, such as R-citalopram and paroxetine.<sup>19,20</sup> However, the advancement in multi-target and allosteric antidepressant drug discovery has been inhibited by the lack of appropriate screening platforms.<sup>1,18</sup> Currently, *in vitro* antidepressant drug discovery is based on electrophysiology, protein phosphorylation assays, and radiolabeled ligand uptake assays. The disadvantages of these methods include time-consuming, labor-intensive experimental work and safety concerns associated with isotope handling.<sup>1</sup>

One strategy to improve the discovery process of novel SNRIs and SNDRIs is the use of fluorescent probes for a target-selective drug screening. However, there are numerous shortcomings when using organic fluorescent probes for drug discovery platforms, for instance limitations in photostability and sensitivity. The emergence of semiconductor nanocrystals, also known as quantum dots (QDs), provided the unique photophysical properties that supplied several advantages which are needed for *in vitro* fluorescence-based studies. QDs are nanometer-sized semiconductor nanocrystals with the exciton Bohr radius smaller than that of the bulk semiconductor material.<sup>9,10</sup> The QDs size tunability of their emission spectra combined with a broad absorption spectra enables and considerably simplifies multiplexing simultaneous imaging of several,

multicolored fluorophores using a single excitation source.<sup>9,10</sup> Compared to traditional fluorophores, the robust inorganic nature of QDs provides excellent photostability and brightness, which allow for long-term imaging of biological systems.<sup>9,10</sup> Previously, research from the Rosenthal group focused on utilizing conjugated QD probes to label SERT in living *Xenopus* oocytes (frog eggs).<sup>18</sup> This labeling approach used ligand-conjugated QD probes that accessed the substrate-binding site and demonstrated a strong model for an *in vitro* drug displacement assay. The ligand construct (IDT318) was designed and synthesized by Ian D. Tomlinson specifically for this study. IDT318 is unique in that it explicitly targets the native substrate (5-HT) binding site via tryptamine drug analogue. However, a drug displacement in an amphibian model does not validate that the ligand-conjugated QD probe can be used in a human model system. In this preliminary report, the ligand-conjugated QD labeling approach for antidepressant drug discovery will be applied to a cellular platform. To use the ligand-conjugated QD labeling approach and ultimately establish antidepressant drug discovery assay in a cell platform, SERT will be labeled with a two-step QD method which allows visualization of the SERT protein. This labeling will result in a distinct, fluorescent signal along the cellular membrane. Using a compact 96-well format, which is suitable for high-throughput drug screening, the labeled fluorescent cells will be treated with SERT selective inhibitors, neurotransmitters, or other potential drug compounds. The selective inhibitors or neurotransmitters, due to high affinity for SERT, will either compete for the protein transporters orthosteric binding site or its secondary, allosteric binding site (Figure 10).

Thus, the SERT selective inhibitor will displace the QD labeled cellular transporter and cause the decrease in fluorescence. There are two possible modes in which the ligand-conjugated QD displacement assay can occur; which are illustrated in Figure 10. The competitive mode (seen on the left) prevents the ligand re-association with the SERT protein primary (or orthosteric) binding site. The allosteric mode (seen on the right) dissociates the ligand through an allosteric mechanism, which cause a conformational change to the primary binding site. The fluorescent measurements will be obtained using the Perkin Elmer Opera™; a premier spinning disk confocal microplate imaging reader for high-throughput high content screening. Based on these aforementioned studies and utilizing cellular response kinetics, selective inhibitors, neurotransmitters or other potential compounds affinities and drug response data will be obtained.

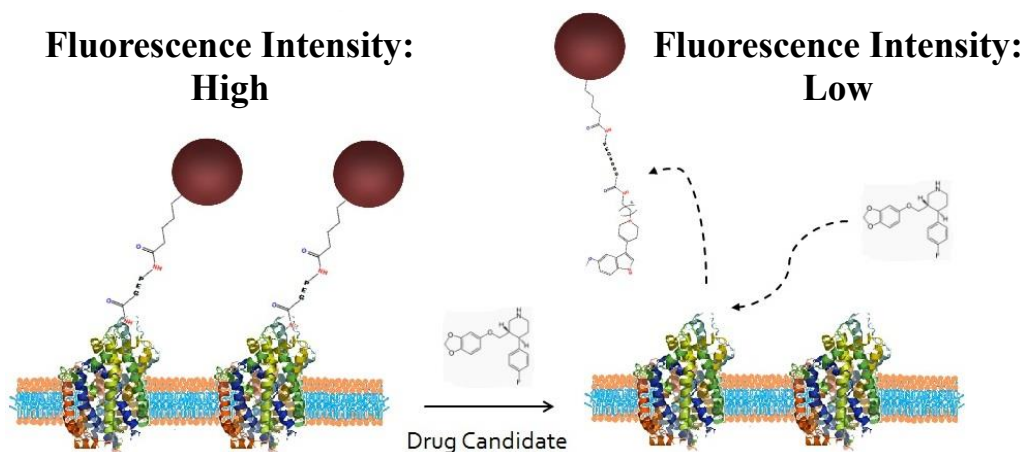


Figure 10. Diagram of QD Based SERT displacement assay



## EXPERIMENTAL

### Fluorescence QD-SERT Ligand Design

The designed ligand IDT318 is composed of four components (as depicted in Figure 11). The IDT318 ligand has the SERT drug analogue, 5-methoxy-3-(1,2,5,6-tetrahydro-4-pyridinyl)-1H-indole (RU24969), which was based on the study of tryptamine derivatives and retains the tryptamine moiety for binding to the common (orthosteric) serotonin binding site (component A).<sup>14,18</sup> The alkyl spacer enhances the ligand binding by allowing the tryptamine moiety an enhanced route to the binding sites (component B). The polyethylene glycol (PEG) chain increases water solubility of the linker and possibly decrease any nonspecific interactions (component C). The biotinylated handle at the end of the PEG chain serves as the binding site for the Streptavidin-Quantum Dots (Streptavidin Qdot® 655, Invitrogen) (component D). The synthetic details of the ligand IDT318 are described in one of our recent publications, where a brief outline is described below.<sup>14,18</sup> The parent drug analogue, 5-methoxy-3-(1,2,5,6-tetrahydro-4-

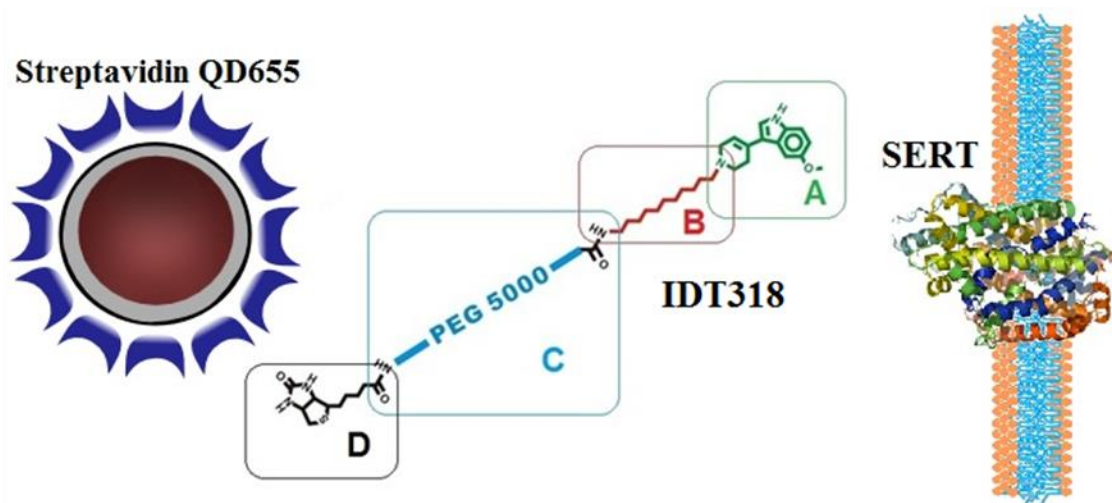


Figure 11. Schematic of Qdot nanoconjugates for SERT labeling. The SERT ligand (IDT318) incorporates a biotin moiety to permit conjugation by SAV-Qdot (D), a PEG chain to reduce steric interference and nonspecific binding (C), an alkyl spacer to provide accessibility to the binding site (B), and a SERT-selective drug derivative, RU24969, to facilitate specific recognition of SERT (A).

pyridinyl)-1H-indole was synthesized and coupled to 11-(1,3-Dioxo-1,3-dihydro-isoindol-2-yl)-undecyl bromide which yields 2-(11-(4-(5-methoxy-1H-indol-3-yl)-5,6-dihydropyridin-(2H)-yl)-undecyl) isoindoline-1,2-dione in the presence of triethylamine. The phthalimide protecting group was removed using hydrazine monohydrate to give 11-(4-(5-methoxy-1H-indol-3-yl)-5,6-dihydropyridin-1(2H)-yl)-undecan-1-amine, which was then coupled to biotin-polyethylene glycol-N-hydroxysuccinimide ester. Once the IDT318 has been synthesized, it can be used as ligand-conjugated probes for a target-selective drug screening

### **Cell Line Maintenance and hSERT Activity Assay**

The hSERT stably transfected HEK293T host cell line was provided by Dr. Randy Blakely's lab (Vanderbilt University) and was grown in complete DMEM, supplemented with 10% dialyzed FBS and incubated in humidified atmosphere with 5% CO<sub>2</sub> at 37°C. The SERT-expressing HEK293T cells were selected in the presence of 400 µg/mL G418.

The SERT protein activity in living HEK293T cells was examined before each experiment by using IDT307, a fluorescent neurotransmitter substrate<sup>15</sup>. IDT307 compound is nonfluorescent in solution but fluoresces as the substrate is accumulated into the nucleus membrane, affording real-time evaluation of SERT uptake activity.<sup>15</sup> The assay to verify successful SERT expression in HEK293T cells involves the addition of IDT307 directly to the culture media at a final concentration of 5 µM and incubating at 37°C for 10 minutes. Fluorescent images were then acquired immediately after IDT307 addition, and successful transporter expression was evident by an observable increase in intracellular fluorescence.

## Labeling HEK293T Cells with Ligand-Conjugated Quantum Dots

To visualize the SERT binding to the ligand-conjugated QD probes in a cellular model, a two-step labeling approach was used. The SERT expressing stably transfected human SERT (hSERT) HEK-293T cell line was chosen as the stable expression system. The cells were grown in 96-well, poly-D-lysine coated, Perkin Elmer Cell Carrier™ plates in 10% dialyzed FBS DMEM media. The stably transfected hSERT HEK-293T cells were treated using a two-step QD labeling protocol. The hSERT-HEK cells were incubated with 0.5  $\mu$ M of the IDT318 ligand in FBS free DMEM media for 10 minutes at 37°C, prior to 5 minute incubation of 1 nM of SavQDs (Qdot® 655 streptavidin conjugate, Invitrogen). After the SavQD655 incubation, several wash steps using fetal bovine serum free containing DMEM media were used to rinse away any unbound ligand and SavQD655s.

### Initial Confocal Fluorescent Microscopy

The initial DIC and fluorescent images were acquired on the Zeiss Laser Scanning Microscope 510 inverted confocal microscope. These initial images were acquired before progressing to the Perkin Elmer Opera™. The microscope excitation source was the 488

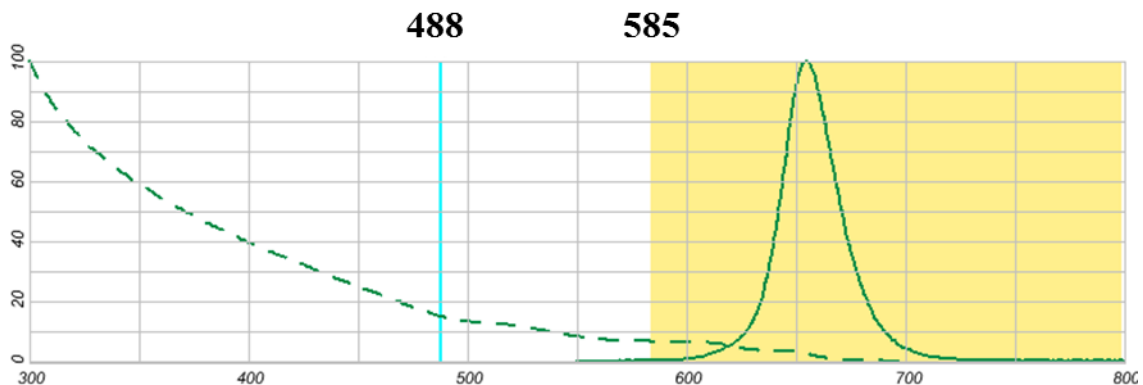


Figure 12. The absorption and fluorescence emission spectra of Qdot® streptavidin conjugate is diagrammed above using the Invitrogen™ Fluorescence SpectraViewer program

nm laser and used a 585 nm long pass filter (Figure 12). Images were attained using the 20X objective and the Zesis Plan-Apo oil immersion objective (63X), with a numerical aperture of 1.40.

## **RESULTS AND DISCUSSION**

When the cells were labeled with the two-step, QD ligand-conjugated method, none of the cells demonstrate the anticipated SERT cell labeling (as seen in Figure 13). In fact, the experimental sample has the same amount of fluorescence as the QD only control (seen in Figure 13). There is uncertainty behind the reason why there is an inability to label and high ligand mediated background. A new batch of IDT318 has been synthesized and is currently being screened for biological functionality (see Appendix C for Ligand screening).

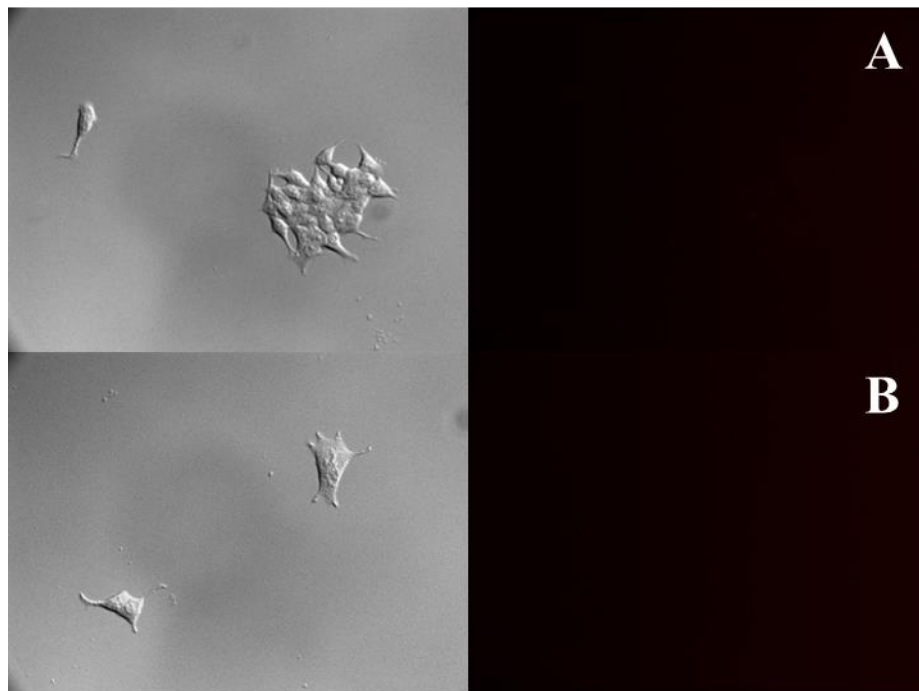


Figure 13-A. Stably transfected hSERT HEK-293T cells treated with 0.5  $\mu\text{M}$  of IDT318 ligand and 1nM of StreptavidinQDs. Panel to the right demonstrates that no labeling was seen using the two-step labeling process.

Figure 13-B. Stably transfected hSERT HEK-293T cells treated with 1nM of StreptavidinQDs only. Panel to the right demonstrates that no Qdot non-specific binding was seen.

As the new batch of IDT318 was being synthesized, a more potent ligand, IDT361, was used to fluorescently label SERT (Figure 14). The ligand IDT361 is approximately one thousand times stronger and more potent than the indole ligand, IDT318.<sup>14,18</sup> The ligand IDT361 includes a cyano derivative on the 5-position of the

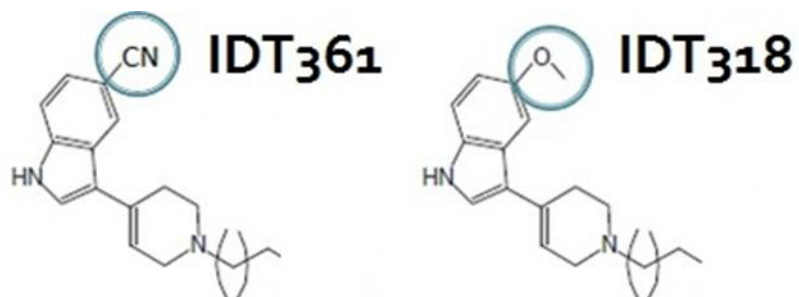


Figure 14. Diagrams of drug analogues of ligands IDT361 and IDT318

indole ring, which allows it to bind stronger than its methoxy group analogue derivative, IDT318.

This stronger binding capability of IDT361 ligand was to demonstrate and visualize the SERT binding to the ligand-conjugated QD probes in the cellular model (Figure 15); IDT361 was less likely to be readily displaced due to its higher affinity for the SERT binding pocket.<sup>14,21</sup> The electrophysiological assay reported in Tomlinson, et. al., supported this by describing a current response induced by the ligands, IDT318 and IDT361, which correlates with the SERT binding affinities of the drug analogues.<sup>22</sup> As indicated, the SERT binding affinity of IDT318 was found to be in low,  $\mu\text{M}$  affinity range; whereas IDT361 had an affinity in the high, nM range.

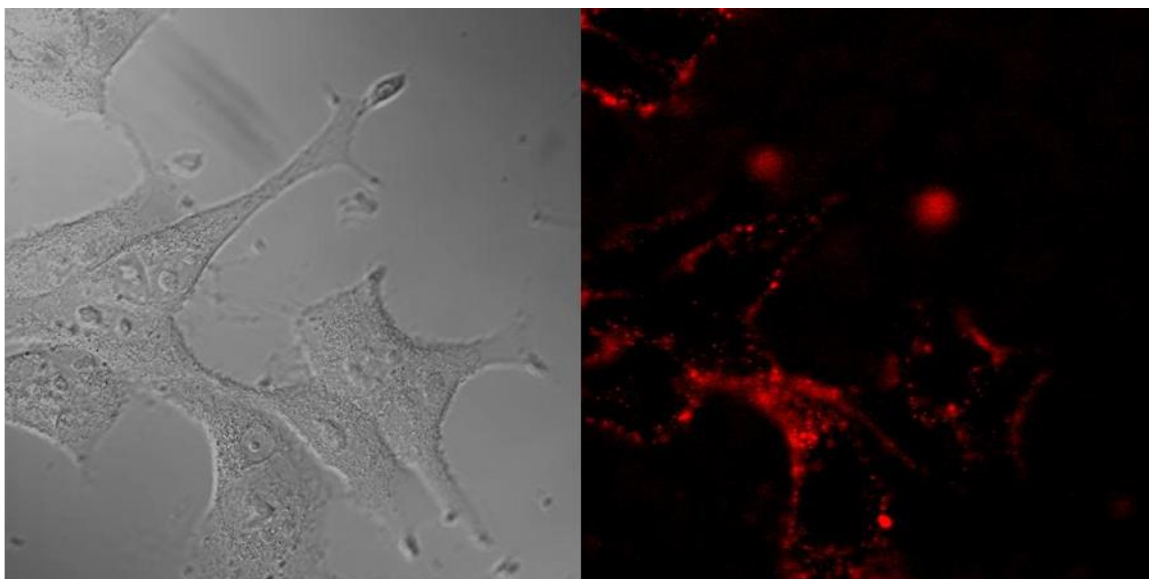


Figure 15. Stably transfected hSERT HEK-293T cells treated with 0.5  $\mu\text{M}$  IDT361 and 1nM of Streptavidin QDots. The panel to the right is the confocal microscopy image of the anticipated labeled cells.

After the two-step labeling method, QD labeled hSERT HEK-293T cells were treated with different concentrations of paroxetine (Paxil®), a high affinity SERT specific inhibitor. As anticipated, the IDT361 was not displaced, as the fluorescence intensity remained constant along the cellular membrane. This is demonstrated in the time-dependent fluorescent intensity plot and images shown below (Figure 16). The IDT361-conjugated QD labeled hSERT HEK-293T cells were treated with 100  $\mu\text{M}$  of the high affinity SERT specific inhibitor, paroxetine. Based on previous publications, the lower affinity IDT318 ligand-conjugated QD probe would be displaced immediately,

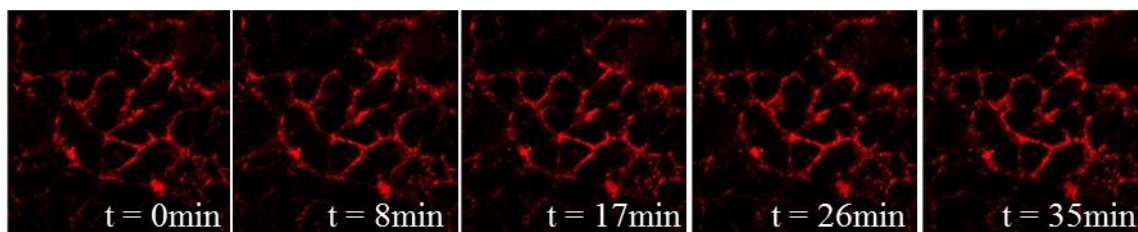
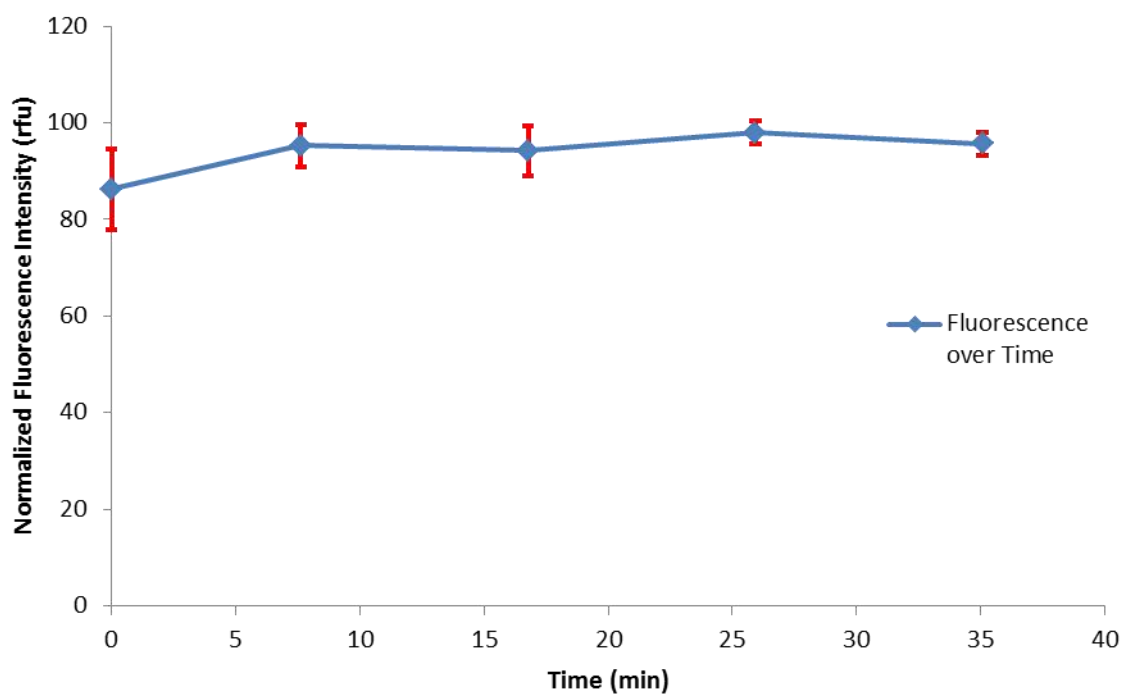


Figure 16. Time-dependent fluorescent intensity plot and images of 100  $\mu\text{M}$  paroxetine treated IDT361-Qdot labeled hSERT HEK-293T cells.

using only 10  $\mu\text{M}$  of paroxetine.<sup>18</sup>

## **CONCLUSION AND FUTURE DIRECTION**

To summarize, our objective is to develop a fluorescence quantum dot SERT displacement assay in a human cellular platform for multi-target drug discovery. Current progress on the SERT displacement assay has demonstrated that using the current batch of IDT318 leads to the inability to label the cells as well as to a high ligand-mediated background. A new batch of IDT318 has been synthesized and is currently being screened for biological functionality (Appendix B). It has also been demonstrated, employing a more potent ligand, IDT361, while able to label the SERT protein, the ligand cannot be displaced using a high affinity SERT specific inhibitor.

The biological functionality of the new batch will be demonstrated using both microscopy and flow cytometry techniques. The stably transfected hSERT HEK-293T cells will be treated with 0.5  $\mu\text{M}$  of the new batch of IDT318 ligand and 1 nM of Streptavidin-QD655 using the two-step labeling approach. The control cell samples will be treated with only 1 nM Streptavidin-QDs without the ligand IDT318. To test for ligand specificity, Paroxetine, a potent and selective serotonin reuptake inhibitor (SSRI), will be used to pre-block the SERT protein. Due to higher fluorescent intensities, the flow cytometry analysis of the ligand-conjugated QD labeled cells, compared with the control samples, will determine cell populations specifically labeled for the SERT protein. After using flow cytometry, the fluorescent microscopy experiments will be performed by simply depositing an aliquot of the cell suspension onto a glass slide and imaging. These approaches can be effective at demonstrating labeling of the SERT protein.



Once the new batch of ligand can be used to label SERT, the ligand-conjugated QD based displacement assay will be demonstrated in the new cellular platform. The cellular displacement assay platform will be tested using SERT selective inhibitors, neurotransmitters, or other potential drug compounds. This new drug discovery assay has the potential to aid in the discovery of new antidepressant and the mapping allosteric versus orthosteric mechanisms of the SERT protein. Once the assay is well established, it will be transitioned to a high-throughput drug screening platform by utilizing the Perkin Elmer Opera™, a premier spinning disk confocal microplate imaging reader.

**B. Human Dopamine Transporter Medium-Throughput Flow Cytometry  
Screening Method**

**INTRODUCTION**

Numerous analytical pharmacological assays methods have been developed to screen for small-molecule modulators or to determine possible target identification and validation of membrane proteins. These pharmacological methodologies are often limited to cell-free assays, which are founded on target-based methods only involving purified enzymes or proteins. These target-based approaches are often based on the assumption that disruption of a single enzymatic reaction or molecular mechanism is the key event in disease ontogeny.<sup>23</sup> More recently, emphasis has been placed on cell-based screens using organic fluorochromes or enzymatic reporters.<sup>24,25</sup> These cell-based systems provide an important approach for investigating quantitative dose response curves that can be generated for a possible high-content analysis. Moreover, cell-based

screens allow the investigation of multiple pathways and many cell types simultaneously.<sup>24,25</sup> While these cell-based assays can provide more detailed data compared to non-cellular based assays, there are still limitations in cell-based assays. Pharmacological screens which focus on a single biochemical target or a single cell type ignore the potential of small molecules or compounds to exhibit differential behavior across cell types and possibly affect multiple signaling pathways.<sup>24,25</sup> The inherent variability of cell types can impede assay design, affect assay robustness, and increase variability from design to design. Even the most advanced live cell-based screens can create assay design issues due to multiple targets across many different cell types.

Therefore, a fluorescence-based platform that can distinguish cell types from one another and simultaneously measure the effects of a drug on multiple pathways in a signaling network would be beneficial.<sup>24,25</sup> Flow cytometry allows for a high-content analysis, multiparameter investigation of a single cell type, making it a promising tool for drug discovery. In these multiparameter approaches, multiple sets of data are collected in a single reaction volume where each data set reports a unique diagnostic component.<sup>26</sup> Here, we present a novel quantum dot based, medium-throughput flow cytometry screening method. To demonstrate this adaptable medium-throughput screening (MTS) method, its properties were utilized in a pharmacological assay.

Nanometer-sized semiconductor nanocrystals, also known as quantum dots (QDs), are nanotechnology's powerful probes and offer a revolutionary fluorescence design. The properties which give QDs their unique aptitudes include: photostability for live-cell imaging and long-term cellular studies, size-tunable color emission, single-excitation source thereby simplifying multicolor analysis, and narrow, symmetrical

emission spectra for low fluorescence cross-talk.<sup>9,10</sup> The possibilities are continually being developed for additional applications of these versatile QDs.<sup>9</sup>

We have previously reported the synthesis and development of ligand-conjugated QD-based systems, employed in the visualization of serotonin transporter, the GABA<sub>A</sub> transporter, and dopamine transporter (DAT).<sup>18,27,28</sup> Our labeling approach used a dopamine transporter with a specific drug end, 2-beta-carbomethoxy-3-beta-(4-fluorophenyl) tropane (IDT44), and biotinylated ligand, which binds to streptavidin-conjugated quantum dots.<sup>27</sup> The ligand, IDT444, utilizes a structural analogue of cocaine, phenyltropane-based dopamine reuptake inhibitor parent compound (beta-CFT, WIN 35,428); which is 3-10x more potent than cocaine and offers excellent labeling stability.<sup>27</sup> Previously, Beta-CFT has been used in the binding of novel ligands to DAT and radioisotope forms of CFT have been used to map the distribution of dopamine transporters in the brain.

In developing our quantum dot based, medium-throughput flow cytometry screening method, our goal is to develop a highly quantitative assay, enabling dose-response titration curves and establish a QD screening assay which had extremely high ability to accurately identify active drug compounds. Furthermore, through the benefit of QDs, our MTS method generates a multipurpose drug screening assay that could measure multi-targets simultaneously and be applied towards the development of drugs beyond the focus of the dopamine transporter.

## EXPERIMENTAL

### Fluorescence QD-DAT Ligand Design

The designed ligand IDT444 is composed of four components (as depicted in Figure 17). The IDT444 ligand has the DAT antagonist, 2- $\beta$ -carbomethoxy-3- $\beta$ -(4-fluorophenyl)tropane, which was based on a cocaine analogue (component A). The alkyl spacer enhances the ligand binding by allowing the cocaine analogue access to the binding sites (component B). The polyethylene glycol (PEG) chain increases water solubility of the linker and possibly decrease any nonspecific interactions (component C). The biotinylated handle at the end of the PEG chain serves as the binding site for the Streptavidin-Quantum Dots (Streptavidin Qdot® 655, Invitrogen) (component D). The synthetic details of the ligand IDT444 are described in one of our recent publications.<sup>27</sup>

### Cell Line Maintenance and hDAT Activity Assay

To visualize the DAT binding to the ligand-conjugated QD probes in a cellular model, a two-step labeling approach was used. The DAT expressing stably transfected

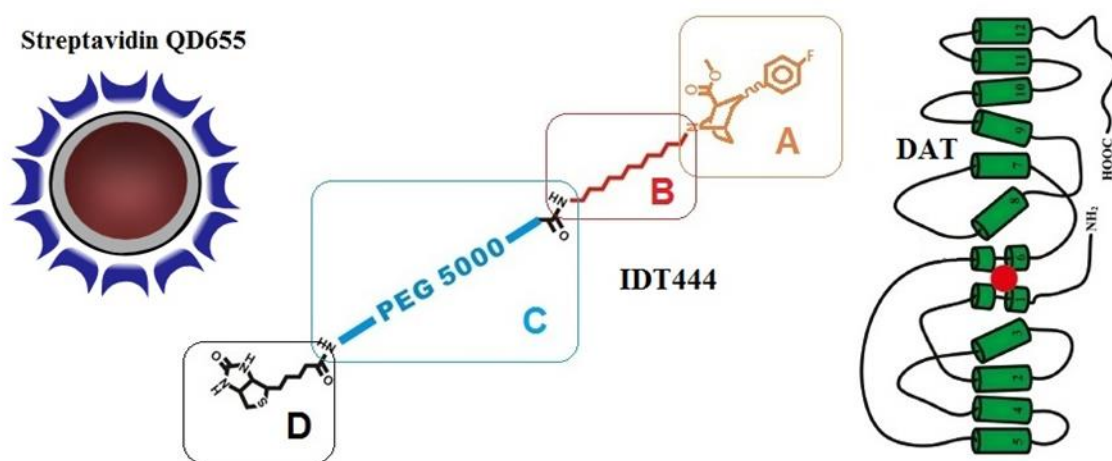


Figure 17. Schematic of Qdot nanoconjugates for DAT labeling. The DAT ligand (IDT444) incorporates a biotin moiety to permit conjugation by SAV-Qdot (D), a PEG chain to reduce steric interference and nonspecific binding (C), an alkyl spacer to provide accessibility to the binding site (B), and a DAT-selective drug derivative,  $\beta$ -CFT or WIN 35,428, to facilitate specific recognition of DAT (A).

human DAT (hDAT) HEK Flp-In-293 cell line was chosen as the stable expression system (obtained from Dr. Randy Blakely's Lab, Vanderbilt University). The cells were grown in complete medium DMEM with L-glutamine, 10% FBS, and 1% pen/strep. The DAT-expressing Flp-In-293 cells were selected in the presence of 100  $\mu\text{g}/\text{mL}$  hygromycin B.

### **Labeling HEK293T Cells with Ligand-Conjugated Quantum Dots for Confocal Fluorescent Microscopy**

The stably transfected hDAT-expressing HEK Flp-In-293 cells were treated using a two-step QD labeling protocol. Previously before imaging experiments, DAT-expressing HEK Flp-In-293 cells were seeded in MatTek (MetTek Corporation) polylysine-coated plates and were allowed to grow for approximately 48 hours at 37°C and 5% CO<sub>2</sub>.

Stably transfected hDAT-expressing HEK Flp-In-293 cells were incubated 37°C and 5%CO<sub>2</sub> for 10 minutes with 100nM of IDT444. Following the ligand incubation, the cells were washed with warm DMEM free media. Once washed, HEK cells were incubated at 37°C and 5%CO<sub>2</sub> for 5 minutes with 1 nM of SavQD655 plus 1%BSA mixture (Qdot® 655 streptavidin conjugate, Invitrogen). After the SavQD655 labeling step, HEK cells were washed with DMEM free media to remove any unbound SavQD655 and cells images were acquired on the Zeiss Laser Scanning Microscope 510 inverted confocal microscope. Images were attained using the 20X objective and the Zesis Plan-Apo oil immersion objective (63X), with a numerical aperture of 1.40.

## **Labeling HEK Flp-In-293 Cells with Ligand-Conjugated Quantum Dots for Flow Cytometry**

The stably transfected hDAT-expressing HEK Flp-In-293 cells were treated using a two-step QD labeling protocol (Figure 18). Prior flow cytometry experiments, DAT-expressing HEK Flp-In-293 cells were seeded in 24-well polylysine-coated plates (BD Bioscience®) and were allowed to grow for approximately 48 hours.

HEK Flp-In-293 cells were washed with warm KRH buffer and incubated with GBR12909, high-affinity DAT antagonist, for 20 minutes at 37°C and 5% CO<sub>2</sub>. HEK cells were then washed again with KRH buffer and incubated at room temperature for 10 minutes with equal parts IDT444 plus GBR12909 in desired concentration mixture or only IDT444 of desired concentration. Following the ligand/drug incubation, the cells were washed with KRH buffer. Once washed, HEK cells were incubated at RT for 5 minutes with 1nM of SavQD655 plus 1% BSA mixture (Qdot® 655 streptavidin conjugate, Invitrogen). After the SavQD655 labeling step, HEK cells were washed with KRH to remove any unbound SavQD655 and cells were nonenzymatically dissociated from the 24-well polylysine-coated plates using CellStripper (Mediatech Inc.) and transferred to polystyrene disposable tubes (BD Bioscience® Falcon tubes).

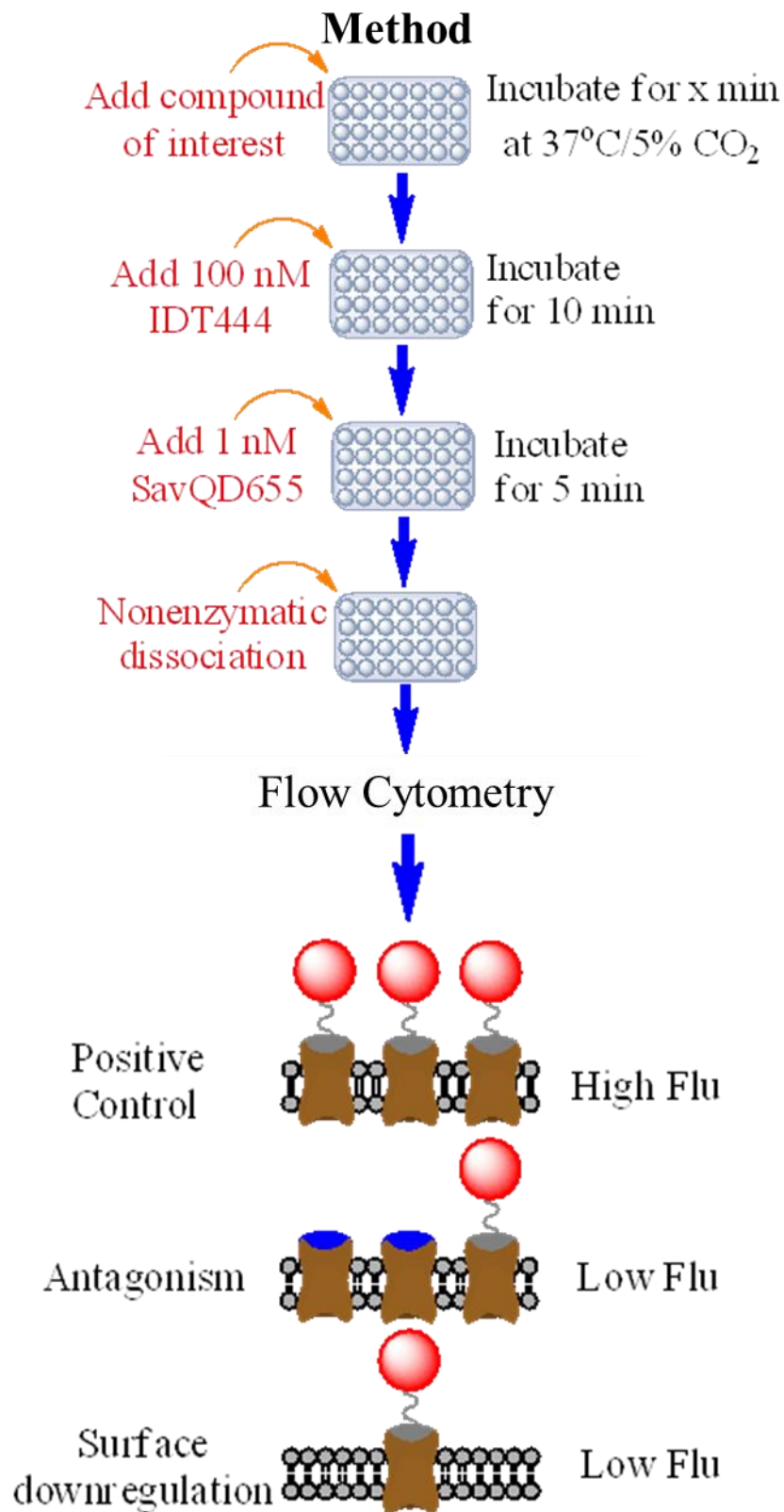


Figure 18. Labeling method of Qdot nanoconjugates for DAT proteins.

## Flow Cytometry

All samples were analyzed on a BD LSRII flow cytometer and the SavQD655 fluorescence was excited at 488-nm excitation laser. Ten thousand events were collected per sample and the median fluorescence intensity (MFI) values were determined for the gated cell fluorescence populations using FlowJo (Tree Star).

## RESULTS AND DISCUSSION

To summarize, our objective is to develop a human dopamine transporter medium-throughput flow cytometry screening assay. Our assay utilizes DAT antagonist-conjugated QDs to assay DAT activity and regulation in live cells in a multi-well plate platform.

Visualization of hDAT HEK293 cells fluorescently labeled with DAT ligand, IDT444 and SavQD655 can be seen in Figure 19. Fluorescent intensities IDT444 Flip In hDAT HEK293 cells positively labeled cells at 20x (B1, B2) and 63x (A1, A2) magnification. Fluorescent (right) and DIC (right) images are shown. Once fluorescent labeling had been demonstrated in the cell line model, the assay's signal dynamic range and evaluation of the quality of this platform, a  $Z'$  statistical factor was determined using only the control data as follows:

$$Z' = 1 - \frac{(3\sigma_{C+} + 3\sigma_{C-})}{|\mu_{C+} - \mu_{C-}|}$$

**Equation 1:  $Z'$  statistical factor**



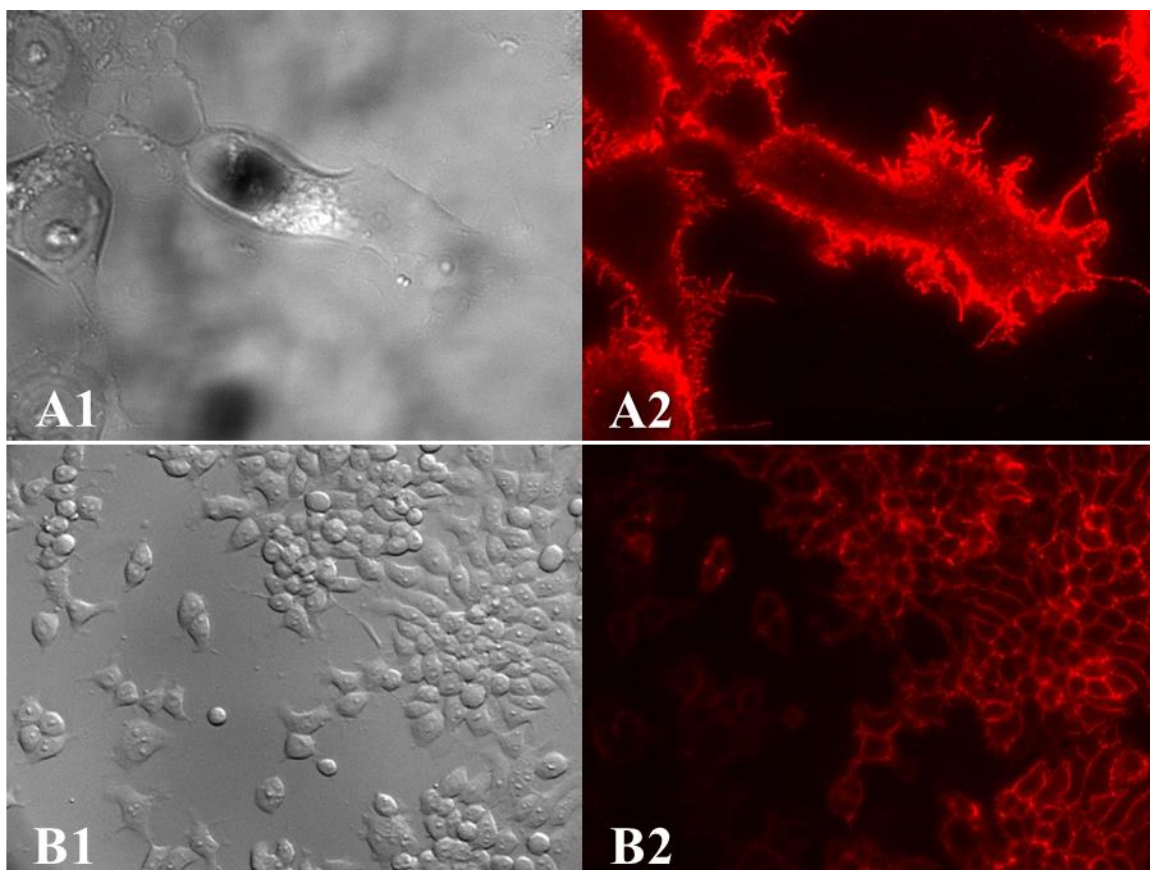


Figure 19. Characteristic images of Flip In hDAT HEK293 cells exposed to two-step SavQD655 labeling protocol using 100 nM concentration of the DAT ligand, IDT444. Fluorescent intensities IDT444 Flip In hDAT HEK293 cells positively labeled cells at 20x (B1, B2) and 63x (A1, A2) magnification. Fluorescent (right) and DIC (right) images are shown.

The  $Z'$ -factor takes into account the signal-to-noise ratio and s.d. of control samples and is commonly utilized for quality assessment in assay development. Values of  $Z' \geq 0.5$  are considered excellent.<sup>29</sup> The  $Z'$ -factor of our QD-based assay was determined to be 0.73, indicating the structure of the assay is of high quality (Figure 20).

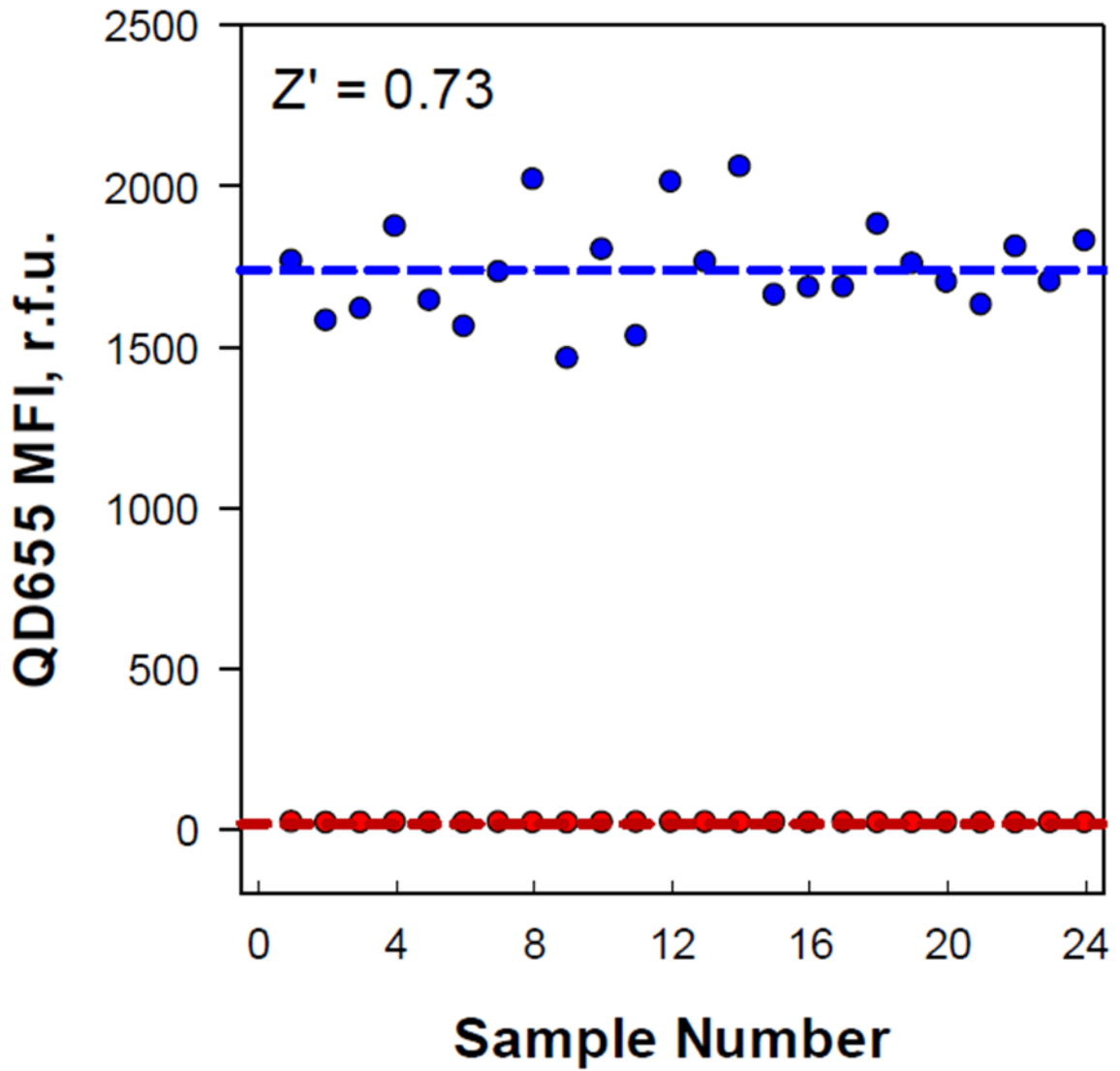


Figure 20. Statistical evaluation, or  $Z'$  factor, of QD-DAT assay quality and repeatability using positive (blue) and negative (red) control data. The Mean MFI is indicated by the dashed lines.

Once the assay validity and quality was determined by the calculated Z'-factor, a series of experiments using a known high-affinity DAT antagonist were performed to evaluate the assay effectiveness. Adherent human DAT-expressing HEK Flp-In-293 cells were exposed to varying GBR12909 antagonist doses. The median fluorescence intensity (MFI) measured by flow cytometry was used to estimate percent inhibition (PI) of QD conjugate binding according to the equation below:

$$PI = \frac{MFI_{pos} - MFI_{treated}}{MFI_{pos} - MFI_{neg}} \times 100\%$$

**Equation 2: Percent Inhibition (PI)**

The obtained PI data were pooled from three independent experiments with triplicate samples to generate a dose-response curve (Figure 21). The half-maximal inhibitory concentration (IC<sub>50</sub>) of GBR12909 was determined to be 27 ± 7 nM, which is in excellent agreement with values obtained using conventional techniques. Typical IC<sub>50</sub> values reported for inhibition of [<sup>3</sup>H]DA transport are in the 1-50 nM range for GBR12909.<sup>30</sup> Together, these experiments demonstrated that our QD-based platform could be used to accurately predict inhibitory activity of DAT antagonist and possibly be used as alternatives for current drug discovery assays.

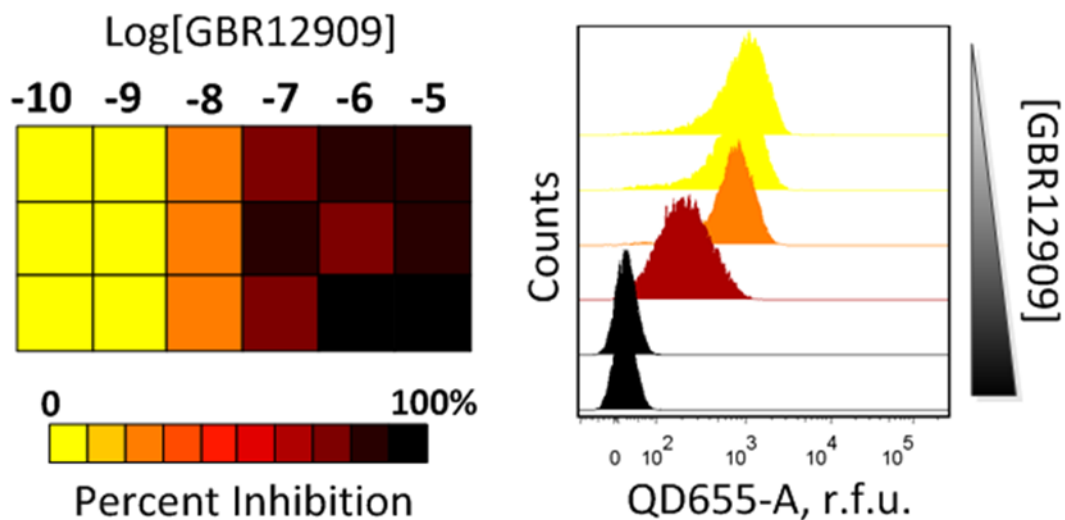


Figure 21. Dose-response screening of GBR12909, high-affinity DAT antagonist, inhibitory activity using antagonist-conjugated QDs. DAT-expressing HEK cells were treated with five- or ten-fold dilutions of GBR12909. Color background box (top left) and histogram plots (top right) of the effects of increasing GBR12909 dose on QD conjugate binding are shown. The IC<sub>50</sub> curve (bottom) was generated from median QD fluorescence intensity values from three independent experiments. Data were fit by sigmoidal dose-response curve, with R<sup>2</sup> = 0.97.

## CONCLUSION AND FUTURE DIRECTIONS

The QD-based flow cytometric assay was used to accurately measure inhibitory action of known high-affinity DAT antagonist, GBR12909. The  $Z'$ -factor, a statistical measure of assay quality and performance, was calculated to be 0.73, which is an “excellent” rating for  $Z'$ -factor. Development of fluorescence-based binding assays that target human cell surface proteins with unresolved crystal structures and ineffective antibodies against the extracellular epitope is particularly challenging.<sup>8</sup> Here, we presented a platform that addresses these issues and could be used as alternative for current drug discovery assays which utilize radioactive materials. Our QD-based assay may also be of potential value to high-throughput of small-molecule neuromodulators of the dopamine transporter, as it can easily employ 384-well plates. In addition, broad absorption and narrow emission spectra of QDs will allow monitoring of several targets or cellular responses and may therefore establish pathway and cell-type selectivity of DAT modulators in a high-content screen.<sup>8,24,25</sup>

## Chapter III

### Development of a Quantum Dot-Based Fluorescent Somatostatin Receptor Probe

#### INTRODUCTION

Somatostatin (SST or SST-14) and the SST receptors (SSRTs) are broadly expressed in the human body where they exert many physiological actions, such as regulating insulin release to modifying the central neural control of blood pressure and breathing.<sup>31-33</sup> The peptide neurotransmitter and hormone somatostatin and the somatostatin receptors (which includes subtypes SSTR1-SSTR5) have been implicated as playing a prominent role in epilepsy. This hypothesis is based on persuasive experimental observations: (1) activity-dependent release of SST peptide during seizures; (2) the modulation of SST mRNA expression, peptide levels and receptors by seizures; (3) the effect of SST and its analogues on seizures in mouse models.<sup>31-35</sup>

In most studies addressing tissue or cell localization and trafficking of the somatostatin receptors, radioactively labeled SST peptide complexes were employed. The intrinsic resolution limit of the radiolabeling approaches precludes capturing these processes with a sufficient level of morphological, functionality, and biomolecular detail.<sup>36</sup>

Questions about the somatostatin system which remain unresolved:

1. Many approaches have been limited and restricted to labeling SST receptors by immunofluorescence techniques. The literature has not begun to explore the labeling

SST ligands and understanding the fate (post-endocytosis) of the peptides *in vitro* and comparing certain cell types.

2. Currently, the literature has not begun to explore the localization, trafficking, and understanding the fate of SST receptors with in an *in vitro* neuronal cells model. This neuronal cell model system would utilize whole cell patch-clamp to induce seizures versus normal neuronal cells.

3. At present, only limited knowledge exists regarding specific interacting proteins which modulate the differential intracellular trafficking of somatostatin receptors. There are big questions remaining about the molecular mechanisms underlying dimerization of the SST protein receptors. It is still debatable if SSTR subunits fit the two general G protein-coupled receptor models (GPCR). Fluorescence tracking data would provide a new level of understanding in the functioning of human SSTRs and may help elucidate the functional properties of GPCR proteins.

Developing and synthesizing a Quantum Dot Somatostatin fluorescence probe would allow us to understand the behavior of the somatostatin receptor subtypes in terms of agonist-induced internalization and receptor interaction and consequently identify somatostatin receptors that should be targeted for future therapeutics.

The emergence of semiconductor nanocrystals, also known as quantum dots (QDs), provided the unique photophysical properties that supplied several advantages which are needed for *in vitro* fluorescence-based studies. QDs are nanometer-sized semiconductor nanocrystals with the exciton Bohr radius smaller than that of the bulk semiconductor material.<sup>9,10</sup> The QDs size tunability of their emission spectra combined with a broad absorption spectra enables and considerably simplifies multiplexing

simultaneous imaging of several, multicolored fluorophores using a single excitation source.<sup>9,10</sup> Compared to traditional fluorophores, the robust inorganic nature of QDs provides excellent photostability and brightness, which allow for long-term imaging of biological systems.<sup>9,10</sup>

By developing and synthesizing a QD somatostatin probe, long-term live-cell imaging can be performed which would allow us to understand the behavior of the somatostatin receptor subtypes in terms of agonist-induced internalization and receptor interaction and consequently identify somatostatin receptors that should be targeted for future therapeutics. Understanding the function of the peptide neurotransmitter/hormone SST and the Somatostatin Receptors (SSTR1-SSTR5), will provide information for clinical therapy for epilepsy, neuroendocrine and metabolic disorders (such as neuroendocrine tumors), retinal disease, and possible medical treatment of schizophrenia disorder.<sup>31-36</sup>

## **EXPERIMENTAL**

### **Materials**

Rink amide resin and Fmoc-protected amino acids, hydroxybenzotriazole (HOBt), 2-(1H-Benzotriazole-1-yl)-1,1,3,3-tetramethylaminium hexafluorophosphate (HBTU), were purchased from Aapptec or AnaSpec. Piperidine, trifluoroacetic acid (TFA), Acetonitrile (HPLC grade), dry diethyl ether, Thioanisole, Ethanedithiol (EDT), Anisole were purchased from Sigma-Aldrich.



## Direct Solid Peptide Synthesis of Somatostatin-14

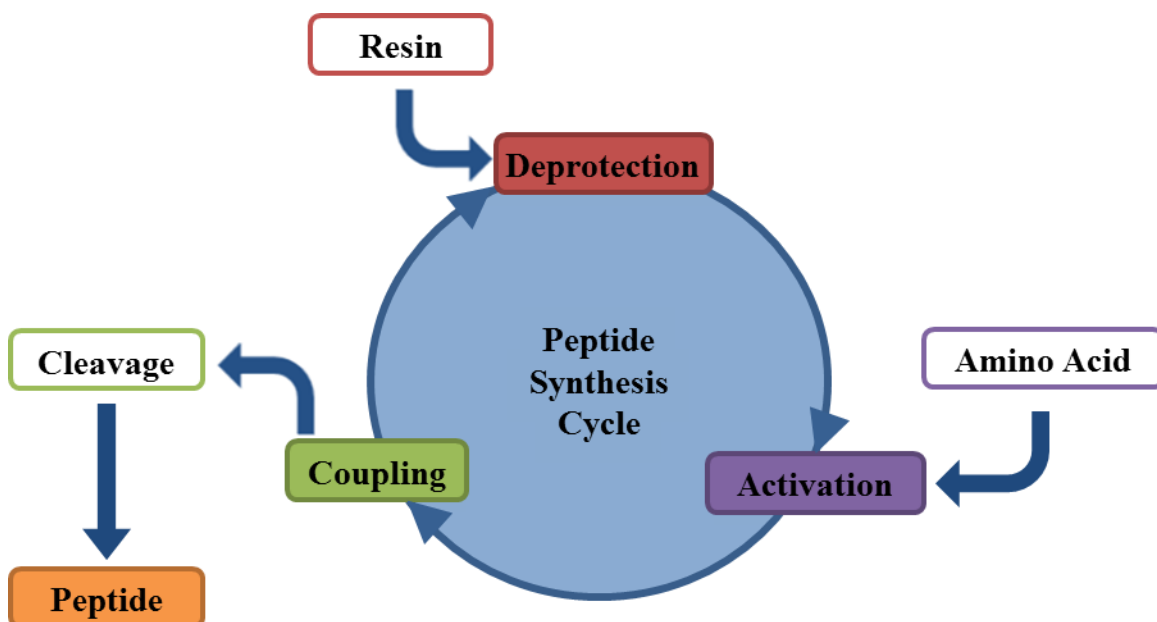


Figure 22. Solid Phase Peptide Synthesis diagram.

Direct solid peptide synthesis of Somatostatin-14 (SST-14) probe was done as described by Jean E. F. Rivier (1974) and Applied Biosystems Technical Bulletin with slight modifications. The sequence of SST-14 was synthesized on Rink amide resin. Resin (0.70 mmol/g) was washed three times with approximately 2 mL of DMF in reaction vessel before starting the synthesis. Coupling was performed by dissolving the Fmoc-protected amino acid with HOBt, HBTU, and DIEA in DMF. After 5 min, the amino acid solution was added to the Rink amide resin and left for 2 hours at 25 °C with continuous swirling. After the final Fmoc deprotection with 20% piperidine in DMF and wash procedure (with DMF, methanol and DMF), the resin complex was dried for deprotection and resin cleavage.

The peptide side chain deprotection and resin cleavage were carried out in Reagent R solution (containing 9.0 mL TFA, 0.5 mL thioanisole, 0.3 mL EDT, and 0.2 mL Anisole) and gently stirred for 2 hours at 25 °C. The peptide was precipitated by addition of ice-cold dry ether, after the removal of Reagent R solution by glass wool filtration. The precipitate was washed with cold ether and lyophilized to white powder. The molecular weight of crude peptide was checked by Matrix-assisted laser desorption/ionization-TOF (MALDI-TOF) and is then purified.

### **High-Performance Liquid Chromatography (HPLC) Purification**

Purification of the SST-14 probe used a reversed-phase C<sub>18</sub> HPLC column. First, an analytical column was used to establish the major peaks, followed by a crude preparation or purification column. The 1 mL of crude peptide (~1 mg/mL) was injected into the HPLC column and eluted with a linear gradient of acetonitrile (from 1% to 80% in 60 min) in 0.1% trifluoroacetic acid (TFA). Peaks were collected at each minute mark between 15 min – 35 min and frozen at -20 °C for later use. When needed, the frozen samples were lyophilized to white powder (if any).

### **Liquid Chromatography-Electrospray Ionization-Mass Spectrometry (LC-ESI MS)**

After the purified HPLC samples were lyophilized, the exact mass of the SST-14 peptide probe was analyzed using Liquid Chromatography-Electrospray Ionization-Mass Spectrometry. The molecular weights of SST-14 probe as well as the purchased SST-14 control from AnaSpec were analyzed.

### **Ellman's Assay**

The Ellman's assay was utilized to verify if the disulfide bond had been formed in the SST-14 peptide probe. In the Ellman's assay, free sulfhydryl groups may be

estimated in the sample by comparing to a cysteine standard. The procedure for quantitation of sulfhydryl groups using a cysteine standard measured at an Absorbance at 412nm and was done as described by Thermo Scientific Ellman's Assay Kit.

## RESULTS AND DISCUSSION

The designed somatostatin probe is composed of three components (as depicted in Figure 23). The SST-14 probe has the Somatostatin peptide, H-Ala-Gly-Cys-Lys-Asn-Phe-Phe-Trp-Lys-Thr-Phe-Thr-Ser-Cys-OH (cyclic, Cys3, Cys14), which was found to bind to the Somatostatin Receptors (which includes all five subtypes, SSTR1-SSTR5) (component A). The Lysine spacer enhances the probe binding by allowing the SST-14 peptide an enhanced route to the Somatostatin receptor binding sites as well as allowing the biotinylated end of the spacer to reach the streptavidin binding pocket (component B).

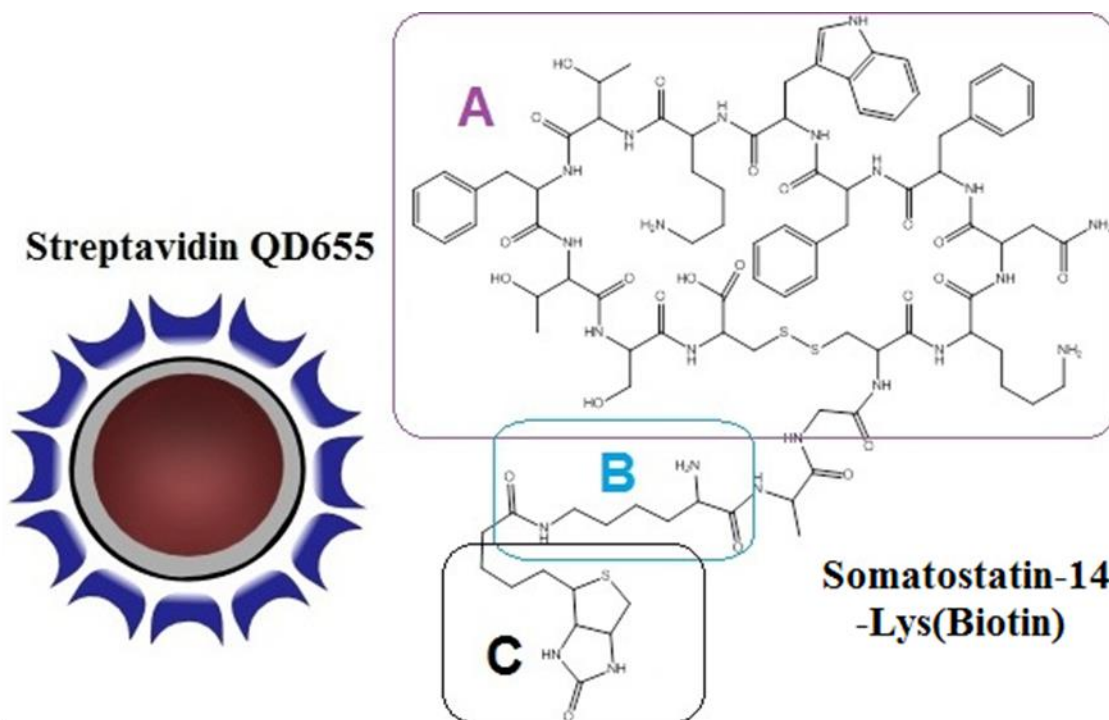


Figure 23. Schematic of Qdot nanoconjugates for Somatostatin receptor (SSTR) labeling. The SST ligand, Somatostatin-14-Lys(Biotin), incorporates a biotin moiety to permit conjugation by SAV-Qdot (C), an lysine spacer to provide accessibility to the binding site (B), and a SST peptide, SST-14, to facilitate specific recognition of SSTR (A).

The biotinylated handle at the alanine end of the peptide serves as the binding site for the Streptavidin-Quantum Dots (Streptavidin Qdot® 655, Invitrogen) (component C).

A schematic representation of the two proposed somatostatin-14, Streptavidin-Quantum Dot probes are depicted in Figure 24.

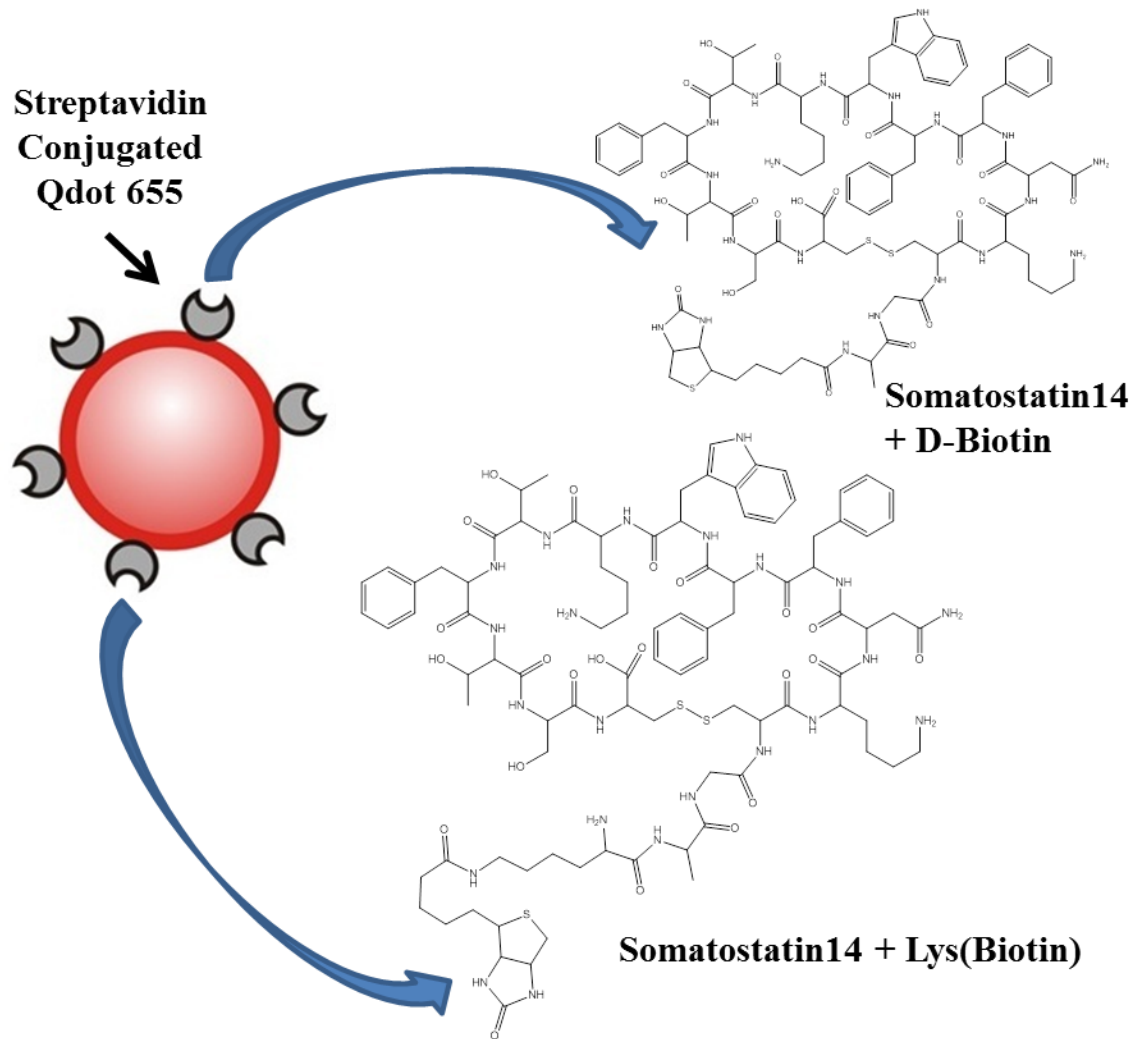


Figure 24. Biotinylated end of the Ala serves as the binding site for the Streptavidin-Quantum Dots (Streptavidin Qdot® 655, Invitrogen)

Based on the literature it was found that the biotin is buried quite deeply inside the streptavidin barrel with the carboxylate oxygens and the ureido-ring nitrogen involved in carboxyl-transfer reactions protruding to the outside. This suggests limits to the nature of conjugating groups for biotin labels used in streptavidin assays.<sup>37-39</sup> The Somatostatin-14-Biotin would most likely not provide the needed length for the biotin to reach inside of the streptavidin binding pocket. Therefore, only one of the two proposed SST-14 Streptavidin Quantum Dot probe, Somatostatin-14-Lys(Biotin), was synthesized by direct solid peptide synthesis (Figure 23)

The 1 mL of crude peptide (~1 mg/mL) was injected and purification of the SST-14 probe used a reversed-phase C<sub>18</sub> HPLC column. An analytical column was used to establish the major peak(s), followed by a crude preparation or purification column. The main peak for both synthesized SST-14 and the Somatostatin-14-Lys(Biotin) probe was seen at ~29 minutes. The main peak in the experimental samples match the control Somatostatin-14 sample purchased from the company AnaSpec. Optical ultraviolet (UV) absorbance of peptides and peptide probes were measured at 280 nm. At this wavelength, the absorbance of peptide is mainly due to the amino acids tryptophan and phenylalanine (see example of UV absorbance in Figure 24).

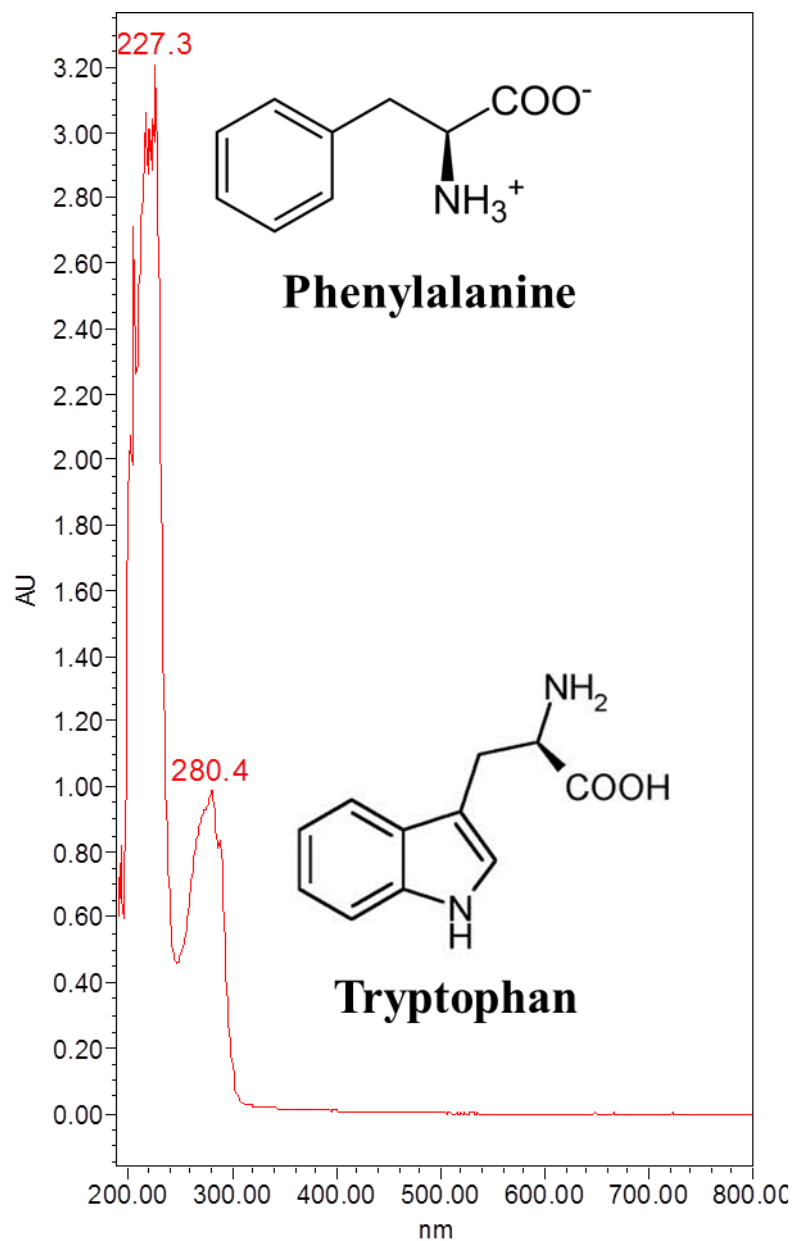


Figure 24. Optical ultraviolet (UV) absorbance of peptides and peptide probes were measured at 280 nm. At this wavelength, the absorbance of peptide is mainly due to the amino acids tryptophan and phenylalanine

After the purified HPLC samples were lyophilized, the exact mass of the purchased Somatostatin -14 control from AnaSpec, SST-14 peptide, and Somatostatin-14-Lys(Biotin) probe were analyzed using Liquid Chromatography-Electrospray Ionization-Mass Spectrometry (LC-ESI MS) in Figures 25 and 26. The predicted

molecular weights for Somatostatin -14 control from AnaSpec and SST-14 peptide was found to be 1637.88 and the molecular weight Somatostatin-14-Lys(Biotin) probe was projected to be 1990.89 using the software program ChemDraw (PerkinElmer). Once analyzed using LC-ESI MS, molecular weights for Somatostatin -14 control from AnaSpec and SST-14 peptide was found to be 1637.71 and 1637.76 respectively. The

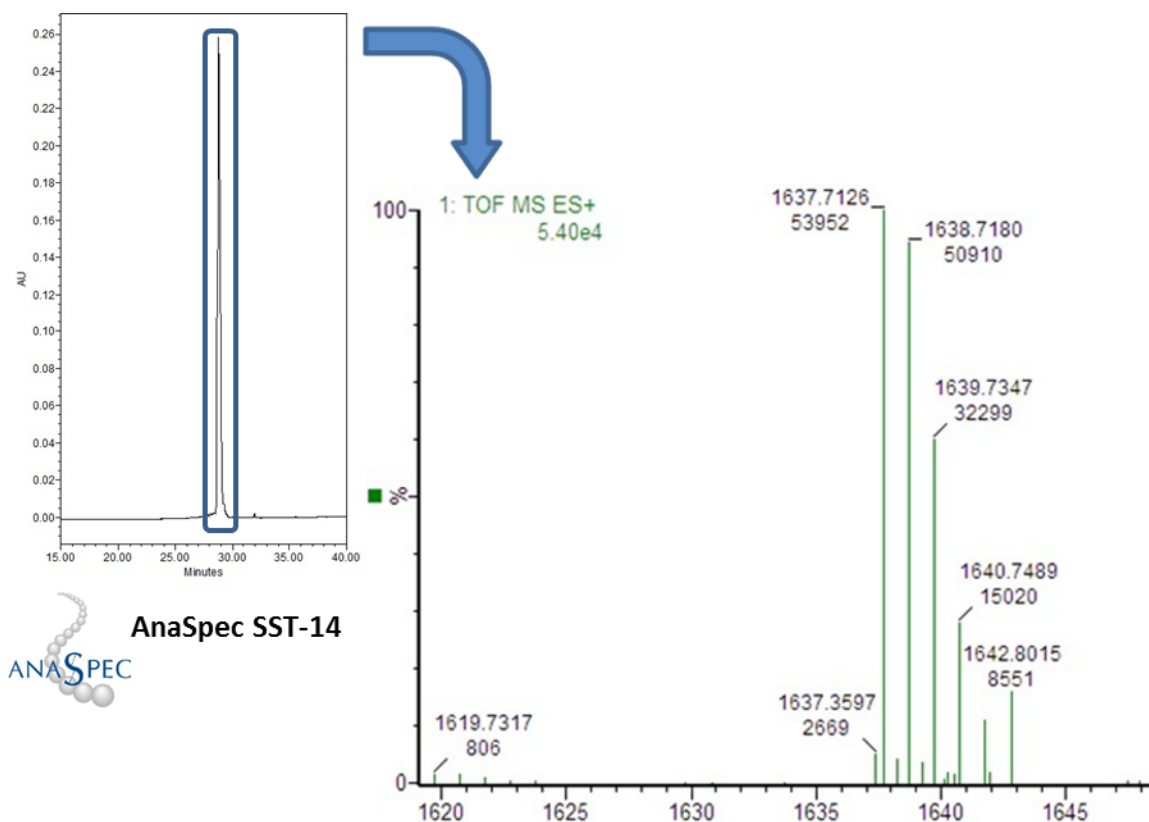
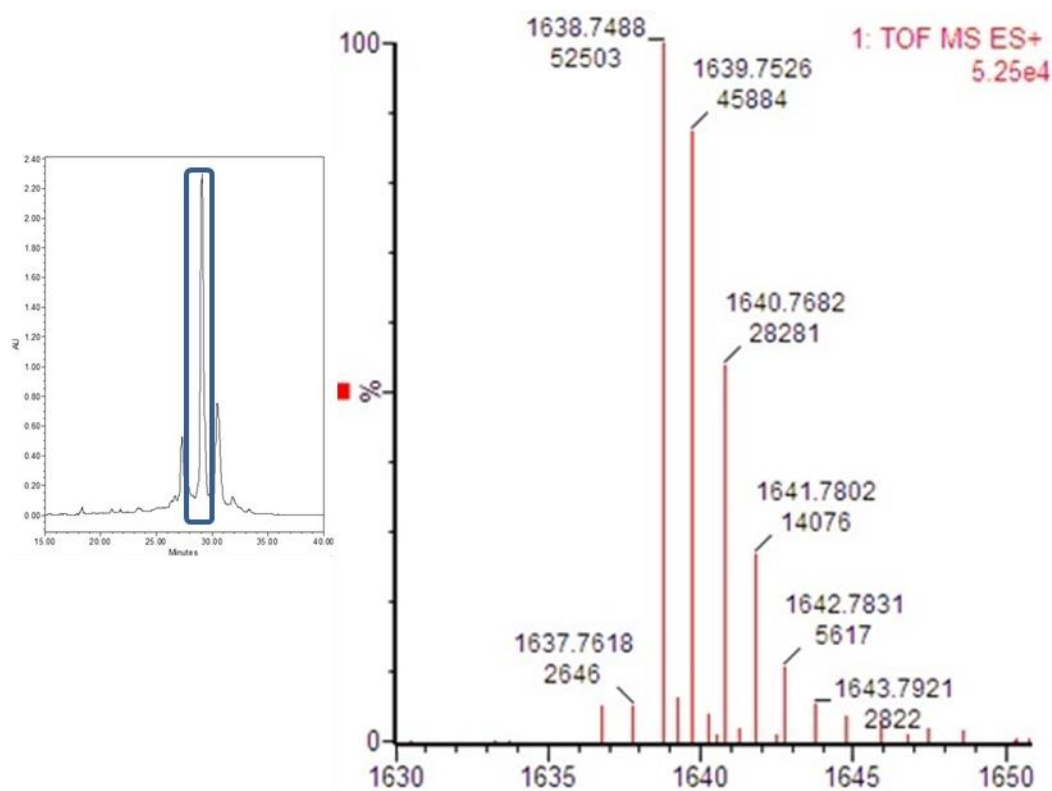
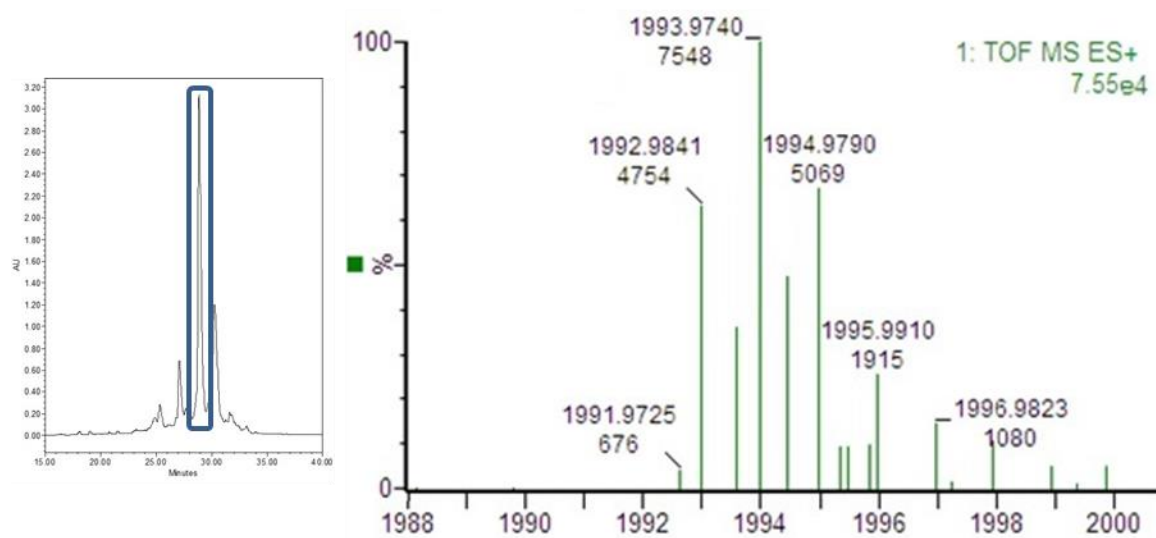


Figure 25. Liquid Chromatography-Electrospray Ionization-Mass Spectrometry (LC-ESI MS) predicted molecular weights for the Somatostatin -14 control from AnaSpec.

molecular weight Somatostatin-14-Lys(Biotin) probe found to be 1991.97, which would probably be characteristic of addition of a hydrogen cation and denoted  $[M + H]^+$ .



### SST-14



### SST-Lys-Biotin

Figure 26. Liquid Chromatography-Electrospray Ionization-Mass Spectrometry (LC-ESI MS) predicted molecular weights for SST-14 peptide and Somatostatin-14-Lys(Biotin) probe



The Ellman's assay was utilized to verify if the disulfide bond had been formed in the SST-14 peptide and Somatostatin-14-Lys(Biotin) probe (see Figure 27). In the

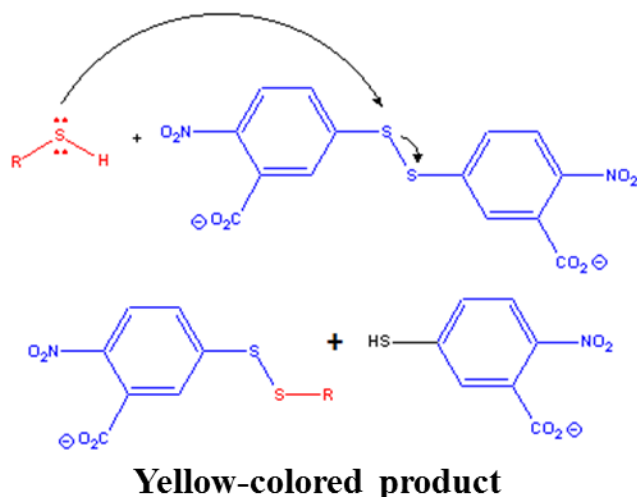


Figure 27. Diagram of Ellman's assay, free sulfhydryl groups may be estimated in the sample by comparing to a cysteine standard

Ellman's assay, free sulfhydryl groups may be estimated in the sample by comparing to a cysteine standard (see Figure 28). The procedure for quantitation sulfhydryl groups using a cysteine standard was done as described by Thermo Scientific Ellman's Assay Kit. Both of the synthesized peptide and probe free sulfhydryl

groups were compared to the purchased Somatostatin -14 control from AnaSpec. Results of Ellman's assay can be seen in Table 1. The purchased Somatostatin -14 control from

AnaSpec had a very low percentage of free sulfhydryl groups (approximately 6%) however, synthesized SST-14

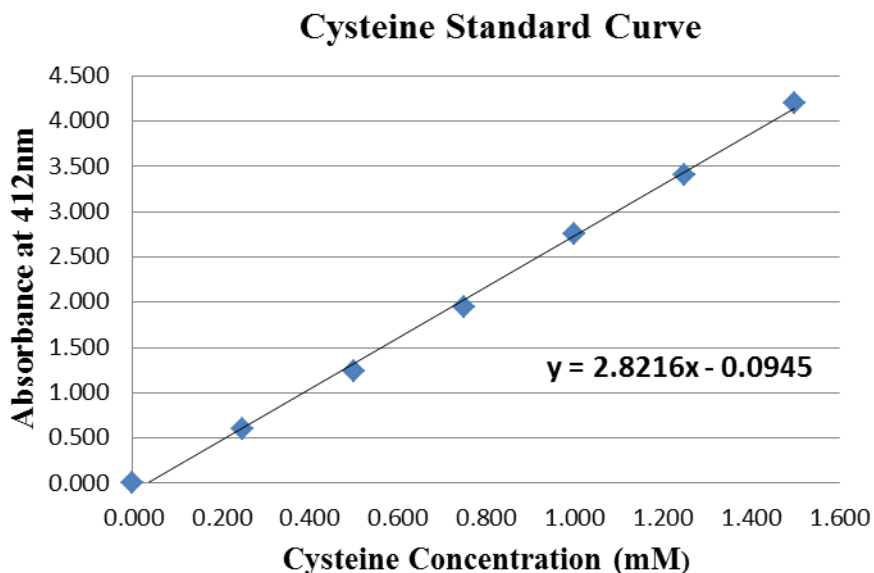


Figure 28. Graph of cysteine standard curve used for the Ellman's assay.

peptide and Somatostatin-14-Lys(Biotin) probe was found to have approximately 33% and 40% respectively. Thus, it is obvious that an oxidation-step needs to be incorporated into the synthesis protocol to increase a complete and better yield.

<b>AnaSpec SST-14</b>	<b>6%</b>
<b>SST-14</b>	<b>33%</b>
<b>Somatostatin-14-Lys(Biotin)</b>	<b>40%</b>

Table 1. Table of results from the Ellman's assay. Synthesized peptide and probe free sulfhydryl groups were compared to the purchased Somatostatin -14 control from AnaSpec.

### **CONCLUSION AND FUTURE DIRECTIONS**

A Somatostatin-14-Lys(Biotin) probe to be used for QD labeling experiments was designed and synthesized. Before cellular testing was performed using transient transfected human somatostatin receptor 2A HEK293T cells, an article from Andrei V. Zvyagin lab was published in Nanomedicine.<sup>40</sup> The author's group report, for the first time, on the development of a quantum dot (QD)-based fluorescent somatostatin probe that enables specific targeting of somatostatin receptors. Receptor-mediated endocytosis of SSTR was imaged using this probe. Once news of the article came to our attention, the Quantum Dot Somatostatin fluorescence probe project was discontinued; there is still opportunity for future studies of fluorescence tracking and localization studies of the

somatostatin receptor subtypes in terms of agonist-induced internalization and receptor interactions.

## **APPENDIX A**

### **Ligand IDT567, IDT571, and IDT576 Screening Process**

#### **INTRODUCTION**

The screening process of ligands: IDT567, IDT571, and IDT576 which contained PEG linkers of 4, 12, and 24 respectively (Figure A-1). The three ligands were synthesized and no further purification methods were completed (such as High-Performance Liquid Chromatography) and molecular weight was never verified by Matrix-Assisted Laser Desorption/Ionization (MALDI).

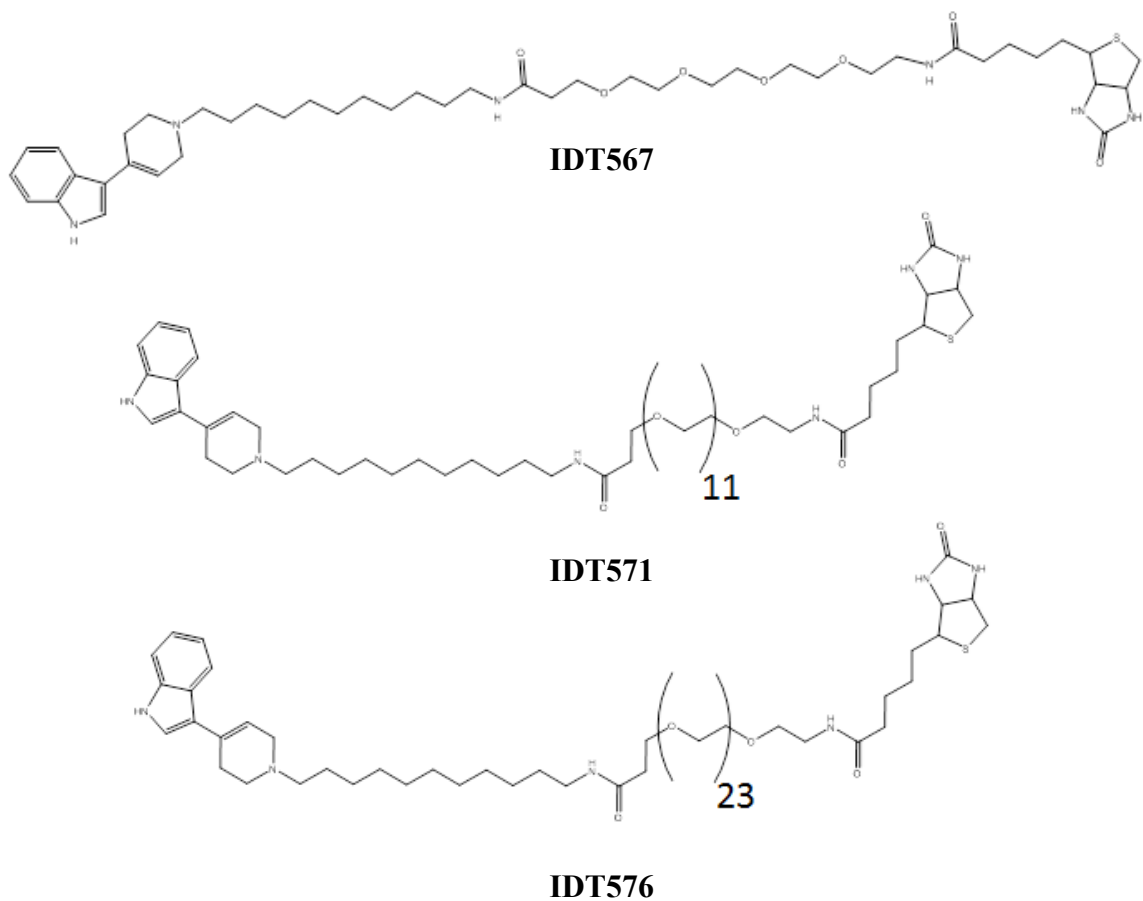


Figure A-1. Ligands IDT567, IDT571, and IDT576

## EXPERIMENTAL

### Cell Line Maintenance and hSERT Activity Assay

The hSERT stably transfected HEK293T host cell line was provided by Dr. Randy Blakely's lab (Vanderbilt University) and was grown in complete DMEM, supplemented with 10% dialyzed FBS and incubated in humidified atmosphere with 5% CO<sub>2</sub> at 37°C. The SERT-expressing HEK293T cells were selected in the presence of 400 µg/mL G418.

The SERT protein activity in living HEK293T cells was examined before each experiment by using IDT307, a fluorescent neurotransmitter substrate.<sup>15</sup> IDT307

compound is nonfluorescent in solution but fluoresces as the substrate is accumulated into the nucleus membrane, affording real-time evaluation of SERT uptake activity.<sup>15</sup> The assay to verify successful SERT expression in HEK293T cells involves the addition of IDT307 directly to the culture media at a final concentration of 5  $\mu\text{M}$  and incubating at 37°C for 10 minutes. Fluorescent images were then acquired immediately after IDT307 addition, and successful transporter expression was evident by an observable increase in intracellular fluorescence.

### **IDT307 Fluorescent Assay**

A 24-well plate was coated with a solution of 0.1% poly-D-lysine. Both hSERT stably transfected HEK293T and HEK293T Wildtype or Sham cells were seeded and grown for 24-48 hours in the 24-well plate until the cells reached a confluence of ~80%. Solutions of IDT567, IDT571, and IDT576 and paroxetine of varying concentrations (0–10 $\mu\text{M}$ ) were prepared by dilution with DMEM-free media (see Figure A-2). Original growth media was aspirated and experimental solutions were added 0.5 mL for each well and incubated for 15 min. Following experimental solution incubation, 5  $\mu\text{M}$  IDT307 was injected into the wells and allowed to incubate for another 10 min. The plate was

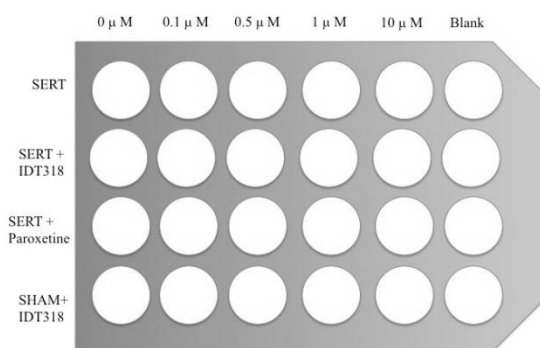


Figure A-2. A sample 24-well plate. Values across the top represent the concentration of drug (IDT318 or paroxetine) added to each well. Images were taken one row at a time to maintain consistency in drug exposure over the course of the experiment.

removed, the media aspirated, and 0.5 mL of fresh DMEM-free was added. The cells were then taken to the fluorescence microscope and images were taken at 20x optical zoom.

## **Labeling HEK293T Cells with Ligand-Conjugated Quantum Dots for Flow Cytometry**

The stably transfected hSERT-expressing HEK293T cells were treated using a two-step quantum dot, Qdot® 655 streptavidin conjugate (Invitrogen™), labeling protocol. Previously before flow cytometry experiments, SERT-expressing HEK293T cells were seeded in 24-well polylysine-coated plates (BD Bioscience®) and were allowed to grow for approximately 48 hours at 5% CO<sub>2</sub> / 37°C. Next, a flow cytometry-based probe screening protocol was established that would allow multi-well plate screening of both adherent and suspension cell cultures using our ligand-conjugated SavQDs. Adherent SERT-expressing (1) competition control cells were pre-blocked by exposure to 10 µM of Paroxetine, a potent and selective serotonin reuptake inhibitor (SSRI), and incubated for 10 minutes at 5% CO<sub>2</sub> / 37°C, (2) competition control, wildtype, and positive cells were incubated with 0.5µM SERT ligands with inhibitor mixture for 10 min for all sample types, (3) washed several times with DMEM free media and incubated with 1 nM SavQD655/1% BSA (bovine serum albumin) mixture, (4) nonenzymatically dissociated (Cellstripper™), and (5) assayed by flow cytometry.

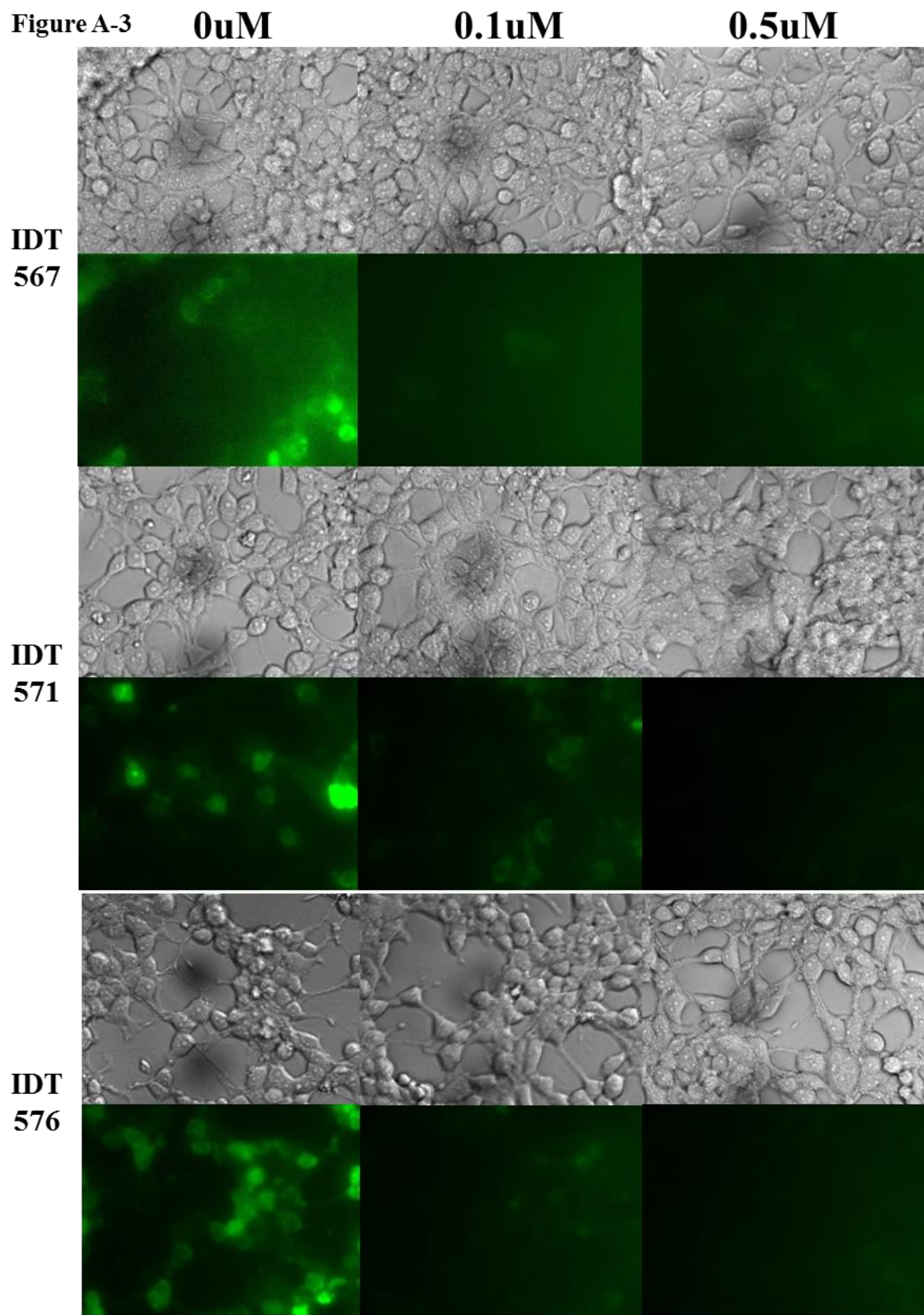
## **RESULTS**

### **IDT307 Fluorescent Assay**

In the fluorescence assay, all three ligands demonstrated the ability to pre-block IDT307 (Figure A-3), a fluorescent neurotransmitter substrate, in concentrations as low as 0.1 µM. It would not be reasonable to assume the pre-blocking ability is solely due to the capability of the IDT ligands. Due to the fact that the drug end of the ligand, 3-(1,2,3,6-tetrahydropyridin-4-yl)-1H-indole, as an IC<sub>50</sub> approximately 0.7 uM,<sup>22</sup> such

strong binding would probably not be exclusively contributed to the ligands. To check this theory, all three ligands were used in the experiment, labeling HEK293T Cells with ligand-conjugated quantum dots for flow cytometry.

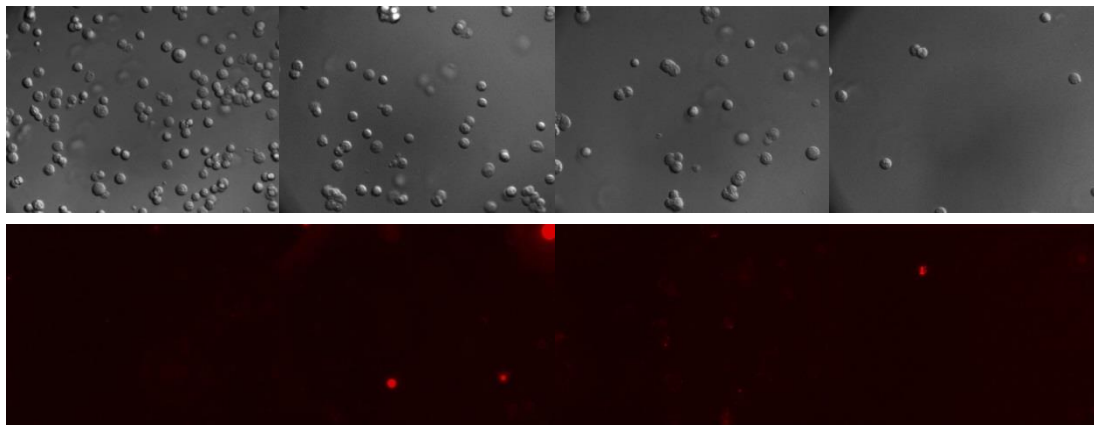




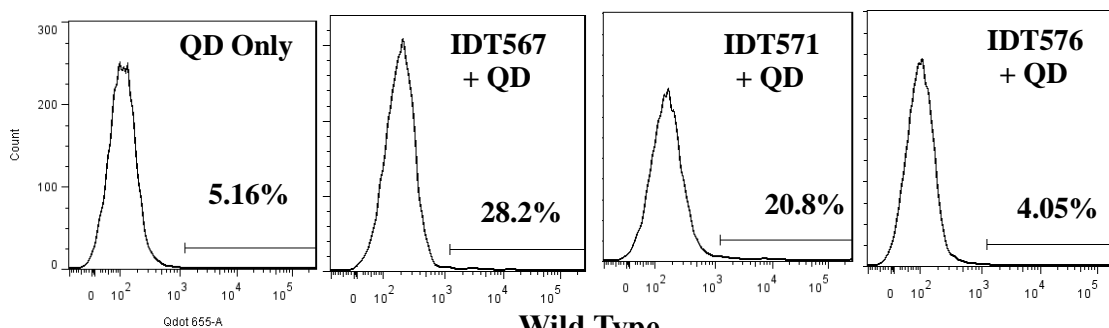
## **Labeling HEK293T Cells with Ligand-Conjugated Quantum Dots for Flow Cytometry**

No specific fluorescence labeling was seen using flow cytometry and microscopy images. The only fluorescence both flow cytometry and microscopy images demonstrated was non-specific QD aggregation (see Figures A-4).

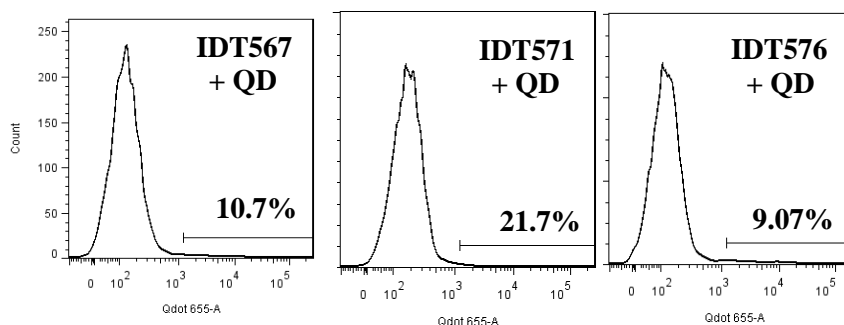
**Figure A-4** **Stably Transfected**



**Stably Transfected**



**Wild Type  
(no SERT)**



## **DISCUSSION**

Even though no specific labeling was seen with the ligands IDT567, IDT571, and IDT576 which contained PEG linkers of 4, 12, and 24 respectively, this does not imply short PEG linkers will not work for future labeling techniques. Rather the lack of labeling is possible due to unknown impurities or synthetic inconsistencies.

## **APPENDIX B**

### **IDT318 Synthesized July 22, 2011 Screened Sept.-Oct., 2011**

#### **INTRODUCTION**

The ligand IDT318 were synthesized and “purification” methods were completed by the ligand passing through a Milipore 3000K column however, High-Performance Liquid Chromatography and molecular weight was verification via Matrix-Assisted Laser Desorption/Ionization (MALDI) was never used.

#### **EXPERIMENTAL**

##### **Cell Line Maintenance and hSERT Activity Assay**

The hSERT stably transfected HEK293T host cell line was provided by Dr. Randy Blakely’s lab (Vanderbilt University) and was grown in complete DMEM, supplemented with 10% dialyzed FBS and incubated in humidified atmosphere with 5% CO<sub>2</sub> at 37°C. The SERT-expressing HEK293T cells were selected in the presence of 400 µg/mL G418.

The SERT protein activity in living HEK293T cells was examined before each experiment by using IDT307, a fluorescent neurotransmitter substrate.<sup>15</sup> IDT307 compound is nonfluorescent in solution but fluoresces as the substrate is accumulated into the nucleus membrane, affording real-time evaluation of SERT uptake activity.<sup>15</sup> The assay to verify successful SERT expression in HEK293T cells involves the addition of IDT307 directly to the culture media at a final concentration of 5 µM and incubating at 37°C for 10 minutes. Fluorescent images were then acquired immediately after IDT307

addition, and successful transporter expression was evident by an observable increase in intracellular fluorescence.

### **IDT307 Fluorescent Assay**

A 24-well plate was coated with a solution of 0.1% poly-D-lysine. Both hSERT stably transfected HEK293T and HEK293T Wildtype (or Sham cells) were seeded and grown for 24-48 hours in the 24-well plate until the cells reached a confluence of ~80%. Solutions of IDT318 and paroxetine of varying concentrations (0–10 $\mu$ M) were prepared by dilution with DMEM-free media (see Figure B-1). Original growth media was aspirated and experimental solutions were added 0.5 mL for each well and incubated for 15 min. Following experimental solution incubation, 5  $\mu$ M IDT307 was injected into the wells and allowed to incubate for another 10 min. The plate was removed, the media aspirated, and 0.5 mL of fresh DMEM-free was added. The cells were then taken to the fluorescence microscope and images were taken at 20x optical zoom.

### **Labeling HEK293T Cells with Ligand-Conjugated Quantum Dots for Flow Cytometry**

The stably transfected hSERT-expressing HEK293T cells were treated using a

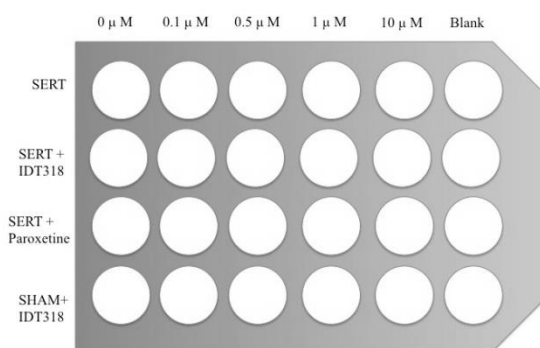


**Figure B-1** sample 24-well plate. Values across the top represent the concentration of drug (IDT318 or paroxetine) added to each well. Images were taken one row at a time to maintain consistency in drug exposure over the course of the experiment.

two-step quantum dot, Qdot® 655 streptavidin conjugate (Invitrogen™), labeling protocol. Previously before flow cytometry experiments, SERT-expressing HEK293T cells were seeded in 24-well polylysine-coated plates (BD Bioscience®) and were

allowed to grow for approximately 48hours at 5% CO<sub>2</sub> / 37°C.

Next, a flow cytometry-based probe screening protocol was established that would allow multi-well plate screening of both adherent and suspension cell cultures using our ligand-conjugated SavQDs. Adherent SERT-expressing (1) competition control cells were pre-blocked by exposure to 10 μM of Paroxetine, a potent and selective serotonin reuptake inhibitor (SSRI), and incubated for 10 minutes at 5% CO<sub>2</sub> / 37°C, (2) competition control, wildtype, and positive cells were incubated with 0.5μM SERT ligands with inhibitor mixture for 10 min for all sample types, (3) washed several times with DMEM free media and incubated with 1 nM SavQD655/1% BSA (bovine serum albumin) mixture, (4) nonenzymatically dissociated (Cellstripper™), and (5) assayed by flow cytometry.

## **RESULTS**

### **IDT307 Fluorescent Assay**

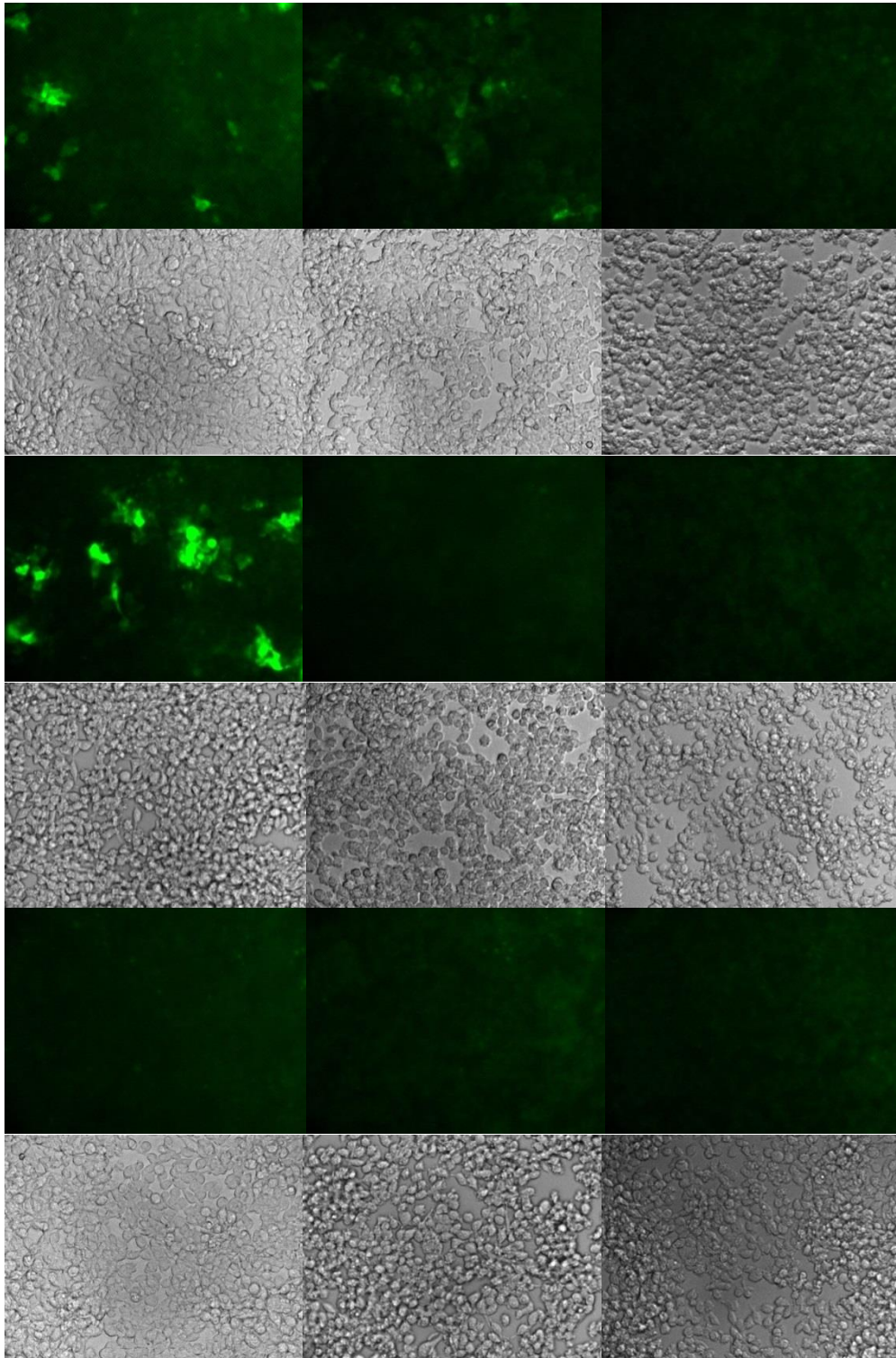
In the fluorescence assay, the ligand demonstrated the ability to pre-block IDT307, a fluorescent neurotransmitter substrate, in concentrations around 1 μM (Figure B-2). Due to the fact that the ligand, IDT318, as an IC<sub>50</sub> of 3.4 uM,<sup>18,21</sup> it was possible that the IDT318 ligand was binding to the SERT protein. To check this theory, all three ligands were used in the experiment, labeling HEK293T Cells with ligand-conjugated quantum dots for flow cytometry.

**0uM**

**1uM**

**10uM**

**Figure B-2**



**ST HEK  
IDT318  
+  
5uM 307**

**ST HEK  
PX pre-  
block  
+  
IDT318  
+  
5uM 307**

**WT HEK  
IDT318  
+  
5uM 307**



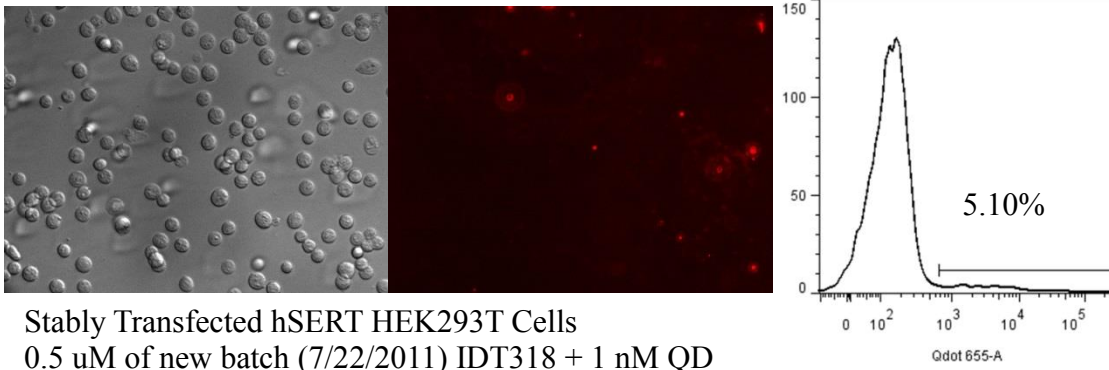
# Labeling HEK293T Cells with Ligand-Conjugated Quantum Dots for Flow Cytometry

## Cytometry

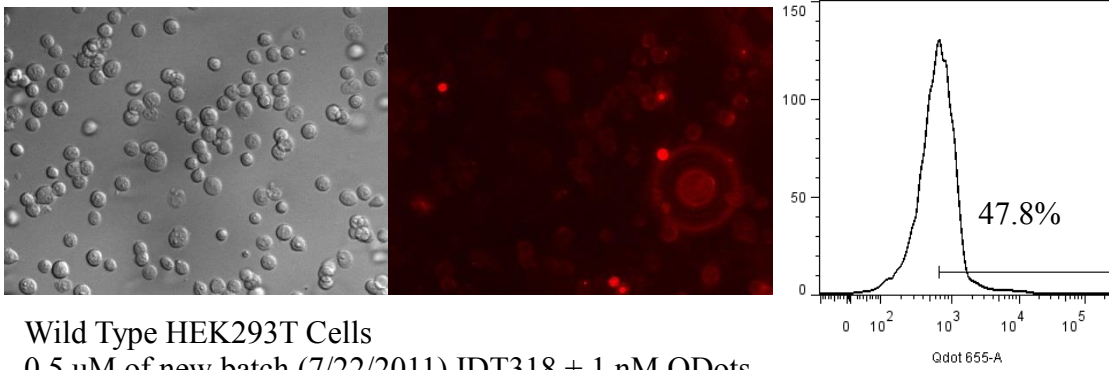
No specific fluorescence labeling was seen using flow cytometry and microscopy images. The only fluorescence both flow cytometry and microscopy images demonstrated was non-specific QD aggregation (see Figures B-3 and B-4).

**Figure B-3**

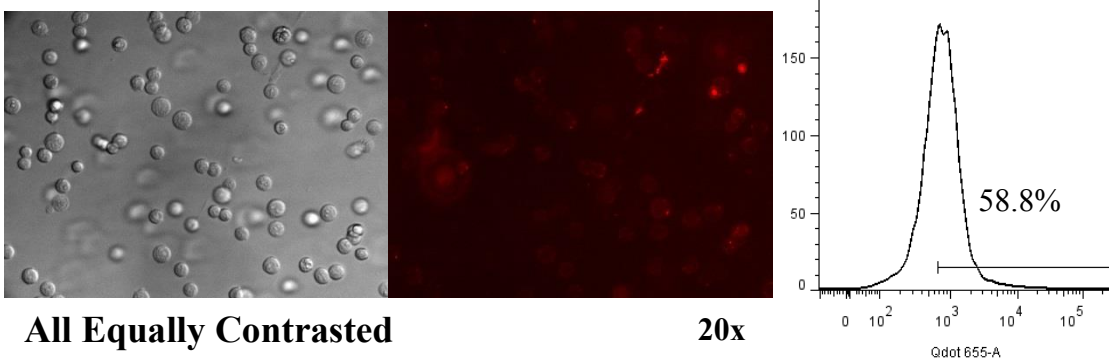
Stably Transfected hSERT HEK293T Cells  
1 nM QD Only



Stably Transfected hSERT HEK293T Cells  
0.5 uM of new batch (7/22/2011) IDT318 + 1 nM QD



Wild Type HEK293T Cells  
0.5 uM of new batch (7/22/2011) IDT318 + 1 nM QDots



All Equally Contrasted

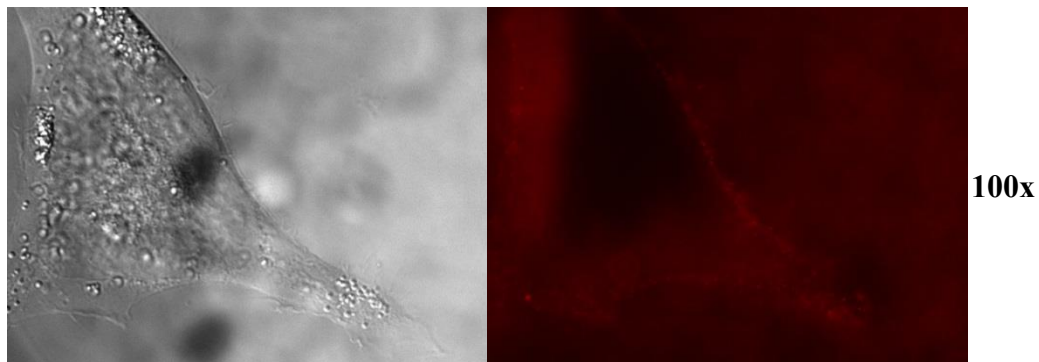
20x



**Figure B-4**

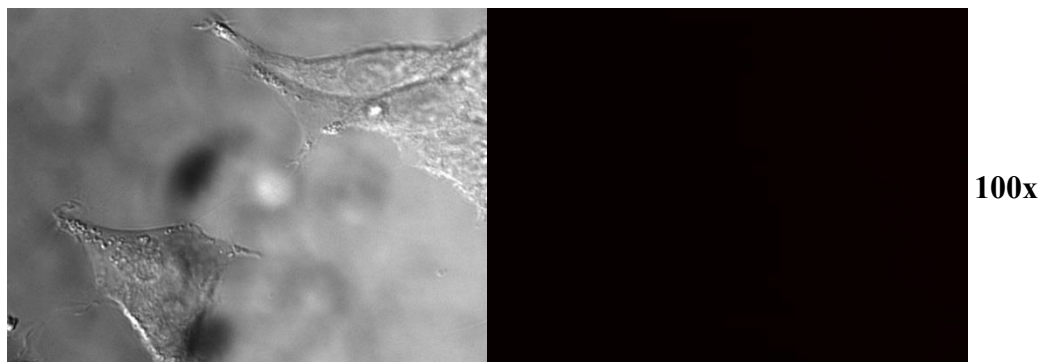
Stably Transfected hSERT HEK293T Cells

**IDT318** 1uM of new batch (7/22/2011) 0.5 uM IDT318 + 1 nM QD



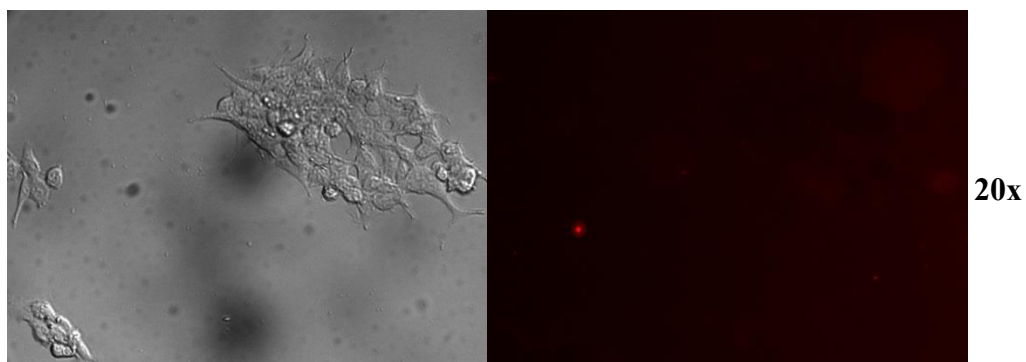
Stably Transfected hSERT HEK293T Cells

**QD only** 1 nM QDots only



Stably Transfected hSERT HEK293T Cells

**IDT318** 1uM of new batch (7/22/2011) 0.5 uM IDT318 + 1 nM QD



**All Equally Contrasted**

## **DISCUSSION**

No specific labeling was seen with the new batch of IDT318 and only non-specific binding was demonstrated.

## APPENDIX C

### Preliminary PerkinElmer Opera Imaging

#### INTRODUCTION

Initial fluorescent visualization using PerkinElmer Opera of the dopamine transporter (DAT) protein in stably expressing Flp-In-293 cells with a custom-made, DAT specific biotinylated ligand, 2- $\beta$ -carbomethoxy-3- $\beta$ -(4-fluorophenyl)tropane (IDT444) that are bound by streptavidin-conjugated quantum dots.

#### EXPERIMENTAL

##### Cell Line Maintenance and hDAT Activity Assay

To visualize the DAT binding to the ligand-conjugated QD probes in a cellular model, a two-step labeling approach was used. The DAT expressing stably transfected human DAT (hDAT) HEK Flp-In-293 cell line was chosen as the stable expression system (obtained from Dr. Randy Blakely's Lab, Vanderbilt University). The cells were grown in complete medium DMEM with L-glutamine, 10% FBS, and 1% penn/strep. The DAT-expressing Flp-In-293 cells were selected in the presence of 100  $\mu$ g/mL hygromycin B.

##### Labeling HEK293T Cells with Ligand-Conjugated Quantum Dots for Confocal PerkinElmer Opera

The stably transfected hDAT-expressing HEK Flp-In-293 cells were treated using a three-step QD labeling protocol. Previously before imaging experiments, DAT-expressing HEK Flp-In-293 cells were seeded in 96-well, poly-D-lysine coated, Perkin

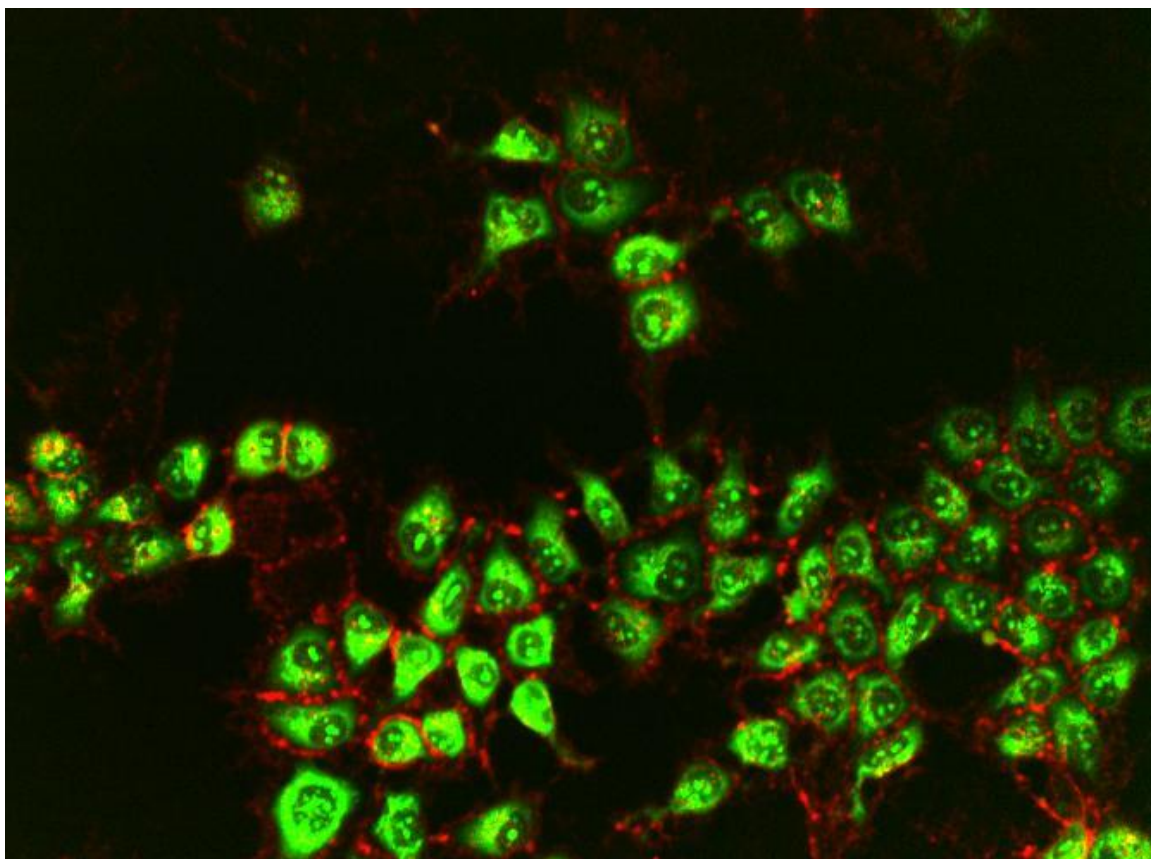
Elmer Cell Carrier™ plates and were allowed to grow for approximately 24 hours at 37°C and 5% CO<sub>2</sub>.

Stably transfected hDAT-expressing HEK Flp-In-293 cells were incubated with 5 μM of IDT307 at 37°C and 5%CO<sub>2</sub> for 10 minutes. After the fluorescent dye incubation, the cells were incubated again at 37°C and 5%CO<sub>2</sub> for 10 minutes with 100nM of IDT444. Following the ligand incubation, the cells were washed with warm DMEM free media. Once washed, HEK cells were incubated at 37°C and 5%CO<sub>2</sub> for 5 minutes with 1 nM of SavQD655 plus 1%BSA mixture (Qdot® 655 streptavidin conjugate, Invitrogen). After the SavQD655 labeling step, HEK cells were washed with DMEM free media to remove any unbound SavQD655 and cells images were acquired on the Perkin Elmer Opera™; a premier spinning disk confocal microplate imaging reader for high-throughput high content screening.

## **RESULTS**

The Perkin Elmer Opera™ appears to be a successful microscope imaging the dopamine transporter (DAT) protein in stably expressing Flp-In-293 cells with the IDT444 ligand bound by streptavidin-conjugated quantum dots (Figure C-1).

**Figure C-1**



## **DISCUSSION**

The Perkin Elmer Opera™ is a good microscope for imaging when there is efficacious ligand labeling.

\

## REFERENCES

1. Milian MJ (2006) Multi-target strategies for the improved treatment of depressive states: Conceptual foundations and neuronal substrates, drug discovery and therapeutic application. *Pharmacol. Ther.*, 110: 135-370
2. Trivedi MH, Desai D, Ossanna MJ, Pritchett YL, Brannan SK, Detke MJ. (2008) Clinical evidence for serotonin and norepinephrine reuptake inhibition of duloxetine. *Int. Clin. Psychopharmacol.*, 23:161–169.
3. Mann JJ (1999) Role of the serotonergic system in the pathogenesis of major depression and suicidal behavior. *Neuropsychopharmacology* 21: 99S-105S
4. Andersen, J., Taboureau, O., Hansen, KB., Olsen, L., Egebjerg, J., Stromgaard, K., Kristensen, AS. (2009) Location of the Antidepressant Binding Site in the Serotonin Transporter: importance of SER-438 in recognition of citalopram and tricyclic antidepressants. *J. Biol. Chem.*, 284(15): 10276-10284
5. Ramsey, IS. and DeFelice LJ. (2002) Serotonin transporter function and pharmacology are sensitive to expression level: evidence for an endogenous regulatory factor. *J Biol Chem*, 277: 14475–14482.
6. Dahan, M., Lévi, S., Luccardini, C., Rostaing, P., Riveau, B., Triller, A. (2003) Diffusion Dynamics of Glycine Receptors Revealed by Single-Quantum Dot Tracking. *Science*, 302: 442-445
7. Fichter, KM., Flajolet, M., Greengard, P., Vu, T. Q. (2010) Kinetics of G-protein–coupled receptor endosomal trafficking pathways revealed by single quantum dots. *Proc. Natl. Acad. Sci. U.S.A.*:107, 18658– 18663

8. Kovtun, O, Ross, EJ, Tomlinson, ID, Rosenthal, SJ, (2012) A flow cytometry-based dopamine transporter binding assay using antagonist-conjugated quantum dots. *Chemical Communications*. 48: 5428-5430.
9. Rosenthal SJ, Chang JC, Kovtun O, McBride JR, Tomlinson ID. (2011) Biocompatible quantum dots for biological applications. *Chemical Chemical Biology*. 18:10-24.
10. Kovtun, O and S. J. Rosenthal, "Biological Applications of Photoluminescent Semiconductor Quantum Dots", in Handbook of Luminescent Semiconductor Materials, Ed. L. Bergman and J. L. McHale, Taylor and Francis Group, New York, 1st edition, 2011, pp. 411–439.
11. Z. Zhou, J. Zhen, N. K. Karpowich, R. M. Goetz, C. J. Law, M. E. A. Reith and D.-N. Wang (2007) LeuT-desipramine structure reveals how antidepressants block neurotransmitter reuptake. *Science* 317, 1390-1393.
12. S. K. Singh, A. Yamashita and E. Gouaux (2007) Antidepressant binding site in a bacterial homologue of neurotransmitter transporters.
13. S. K. Singh (2008) LeuT. *Channels* 2, 380-389.
14. Tomlinson ID, Iwamoto H, Blakely RD, Rosenthal SJ. (2011) Biotin tethered homotryptamine derivatives: High affinity probes of the human serotonin transporter (hSERT). *Bioorg Med Chem Lett* 21: 1678-1682.
15. Solis, E Jr, Zdravkovic, I, Tomlinson, ID, Noskov, SY, Rosenthal, SJ, De Felice, LJ. (2012) 4-(4-(dimethylamino)phenyl)-1-methylpyridinium (APP+) is a fluorescent substrate for the human serotonin transporter. *J Biol Chem*. 287:8852-63.

16. Starr KR, Price, GW, Watson, JM, Atkinson, PJ, Arban, R, Melotto, S, Dawson, LA, Hagan, JJ, Upton, N, and Mark S Duxon, MS. (2007) SB-649915-B, a Novel 5-HT<sub>1A/B</sub> Autoreceptor Antagonist and Serotonin Reuptake Inhibitor, is Anxiolytic and Displays Fast Onset Activity in the Rat High Light Social Interaction Test. *Neuropsychopharmacology* 32: 2163-2172
17. Yamashita, A, Singh, SK, Kawate, T, Jin, Y, Gouaux, E. (2005) Crystal structure of a bacterial homologue of Na<sup>+</sup>/Cl<sup>-</sup>-dependent neurotransmitter transporters. *Nature*. 437:215-23.
18. Chang JC, Tomlinson ID, Warnement MR, Iwamoto H, DeFelice LJ, Blakely RD, Rosenthal SJ. (2011) A Fluorescence Displacement Assay for Antidepressant Drug Discovery Based on Ligand-Conjugated Quantum Dots. *Journal of The American Chemical Society*. 133: 17528-17531.
19. S Mager, C Min, Henry DJ, C Chavkin, Hoffman BJ, N Davidson, Lester HA. (1994) Conducting states of a mammalian serotonin transporter. *Neuron* 12:845–859
20. Mnie-Filali, O, et. al. (2007) *Encephale* 33(6):965-72
21. Tomlinson ID, Warnerment, MR, Mason, JA, Vergne, MJ, Hercules, DM, Blakely RD, Rosenthal SJ. (2007) Synthesis and characterization of a pegylated derivative of 3-(1,2,3,6-tetrahydro-pyridin-4yl)-1H-indole (IDT199):A high affinity SERT ligand for conjugation to quantum dots. *Bioorg Med Chem Lett* 17: 5656–5660.
22. Deskus, JA, et. al. (2007) *Bioorg. Med. Chem. Lett.* 17:3099-3104



23. Lang P, Yeow K, Nichols A, Scheer A (2006) Cellular imaging in drug discovery. *Nat Rev Drug Discov* 5:343-356.
24. Krutzik, PO, Nolan, GP. (2003) Intracellular phospho-protein staining techniques for flow cytometry: monitoring single cell signaling events. *Cytometry A* 55, 61
25. Krutzik, PO, Crane, JM, Clutter, MR, Nolan, GP. (2008). High-content single-cell drug screening with phosphospecific flow cytometry. *Nat. Chem. Biol.* 4, 132
26. Edwards, BS, Young, SM, Saunders, MJ, Bologna, C, Oprea, IT, Ye, RD, Prossnitz, ER, Graves, SW, and Skla, LA.(2007) High-throughput flow cytometry for drug discovery. *Expert Opin. Drug Discov.* 2:1-12
27. Kovtun O, Tomlinson ID, Sakrikar DS, Chang JC, Blakely RD, Rosenthal SJ. (2011) Visualization of the Cocaine-Sensitive Dopamine Transporter with Ligand-Conjugated Quantum Dots. *ACS Chemical Neuroscience.* 2: 370-378.
28. Tomlinson, ID, Gussin, HA, Little, DM, Warnement, MR, Qian, H, Pepperberg, DR, and Rosenthal, SJ. (2007) Imaging GABA<sub>A</sub> Receptors with Ligand-Conjugated Quantum Dots. *J Biomed Biotechnol.* 76514.
29. J.-H. Zhang, T. D. Y. Chung and K. R. Oldenburg, (1999) *J. Biomol. Screening*, 4(2), 67–73.
30. E. Hosli and L. Hosli, (1997) Expression of GABA(A) receptors by reactive astrocytes in explant and primary cultures of rat CNS. *Int. J. Dev. Neurosci.*, 15: 949-60
31. Srikant, CB; et al. (2004) *Somatostatin*. Springer
32. Bronstein-Sitton, N. (2006) Somatostatin and the Somatostatin Receptors: Versatile Regulators of Biological Activity. *Pathways*

33. Jacobs, S. and Stefan Schulz. (2008) Intracellular Trafficking of Somatostatin Receptors. *Molecular and Cellular Endocrinology*. 286:58-62
34. Tallent, MK, and Qiu C (2008) Somatostatin: An endogenous antiepileptic. *Molecular and Cellular Endocrinology*. 286: 96–103
35. Qiu, C, Zeyda, T, Johnson, B, Hochgeschwender, U, Luis de Lecea, and Tallent, MK. (2008) Somatostatin Receptor Subtype 4 Couples to the M-Current to Regulate Seizures. *The Journal of Neuroscience*. 28(14):3567-3576
36. Varun K. A. Sreenivasan, Oleg A. Stremovskiy, Timothy A. Kelf, Marika Heblinski, Ann K. Goodchild, Mark Connor, Sergey M. Deyev, and Andrei V. Zvyagin. (2011) Pharmacological Characterization of a Recombinant, Fluorescent Somatostatin Receptor Agonist. *Bioconjugate Chem*. 22:1768–1775
37. Hendrickson, WA, Pähler, A, Smith, JL, Satow, Y, Merritt, EA, and Phizackerley, RP. (1989) Crystal structure of core streptavidin determined from multiwavelength anomalous diffraction of synchrotron radiation. *Proc Natl Acad Sci U S A* 86(7): 2190–2194.
38. Weber, PC, Ohlendorf, DH, Wendoloski, JJ, Salemme, FR. (1989) Structural origins of high-affinity biotin binding to streptavidin. *Science* 243(4887):85-8.
39. Claire E. Chivers, Apurba L. Koner, Edward D. Lowe et al., (2011). How the biotin-streptavidin interaction was made even stronger: investigation via crystallography and a chimaeric tetramer. *Biochemical Journal*, 435, 55-63.
40. Varun KA Sreenivasan , Eun J Kim , Ann K Goodchild , Mark Connor , Andrei V Zvyagin. (2012) Targeting somatostatin receptors using in situ-bioconjugated fluorescent nanoparticles. *Nanomedicine*. 7(10):1551-1560.